

MARGINAL GAP AND INTERNAL FIT OF A ZIRCONIA CROWN  
AND IMPLANT ABUTMENT USING THREE DIFFERENT DIGITAL  
WORKFLOWS

A Thesis

By

STEPHANIE KAYLEEN ZELLER

Submitted to the Office of Graduate and Professional Studies of  
Texas A&M University  
in partial fulfillment of the requirements for the degree of

MASTER OF SCIENCE

Chair of Committee,  
Committee Members,  
Head of Department,

William W. Nagy  
Elias Kontogiorgos  
Jorge Gonzalez  
Larry Bellinger

May 2017

Major Subject: Oral Biology

Copyright 2017 Stephanie Zeller

## ABSTRACT

Computer-assisted design (CAD) and computer-assisted manufacturing (CAM) have been gaining widespread acceptance and use in implant dentistry. Due to rapidly accelerated growth, few digital workflows utilizing CAD/CAM technology for implant restoration fabrication have been evaluated. The aim of this study was to evaluate marginal and internal adaptation of an implant abutment and crown using three digital workflows. The first workflow, the more traditional interrupted digital workflow which includes a re-scan of the final abutment, was compared to two full digital workflows, using the 3Shape split-file and Atlantis core-file.

Group 1, “Interrupted Digital Atlantis Workflow”, represented the most utilized customary workflow, which included a customized Atlantis abutment that was designed and received, and then re-scanned for final crown design. Group 2, “Full Digital Atlantis Workflow”, included a customized Atlantis abutment and its corresponding .STL, the Atlantis Core File, which was immediately imported into design software and used for crown design and milling. Group 3, “Full Digital Split-File Workflow”, utilized 3Shape’s full digital workflow for abutment and crown design called the split-file workflow. All crowns for the study were zirconia milled with a 5-axis mill.

Marginal opening, marginal gap and internal fit were evaluated for all three groups using two forms of measurement, first by sectioning the specimens and evaluating them with a Scanning Electron Microscope (SEM). Secondly by a silicone replica technique and Geomagic software. Group results were compared while concurrently validating the Geomagic measuring protocol as outlined within the study.

A Kruskal-Wallis test was administered followed by post-hoc Mann-Whitney tests with Bonferroni correction of  $p < 0.017$ , adjusting for multiple comparisons. A statistically significant difference was found for SEM marginal opening Group 3 Full Digital Split-File (0.002), showing a significantly larger marginal gap compared to both Groups 1 and 2. SEM marginal gap Group 2 Full Digital Atlantis was statistically smaller (0.002) than both Groups 1 and 3. Similar to SEM marginal gap measurement comparisons, Geomagic marginal gap comparisons indicated Group 2 Full Digital Atlantis was statistically smaller from Group 1 (0.004) and Group 3 (0.006). Geomagic internal fit comparisons indicated Group 3 was statistically larger (0.006) than both Groups 1 and 2. Geomagic validation was completed with two separate paired t-test evaluations, both indicating no significant differences between SEM measurements and Geomagic, concluding Geomagic measuring protocol herein to be a valid means of measurement.

The observed results yield multiple conclusions. All three workflows evaluated showed clinically acceptable results. SEM evaluation of marginal opening revealed the two Atlantis Groups 1 and 2 to have smaller openings than Group 3 Split-file. SEM and Geomagic marginal gap evaluation revealed the Group 2 Full Digital Atlantis group to have the smallest gap. Geomagic internal fit evaluation revealed a smaller internal fit for Group 3 Splitfile. In addition, statistical results of SEM and Silicone-Replica Geomagic measuring technique revealed the Geomagic measuring protocol to be a valid form of measurement.

## DEDICATION

I would like to dedicate this work to my husband, Mike. Thank you for your unwavering support and love throughout this process. I would not be who I am today without you. I love you.

To my parents, Stephen and Kathy, thank you for your wisdom, guidance, love and support, not just throughout this process, but throughout my entire life. You have shown me what it looks like to be tremendously selfless and loving, gracious parents.

To my sisters, Caroline and Gabby, thank you for being an amazing foundation of love and consistency within my life and throughout this process. To my brother, thank you for your consistent calming support.



## ACKNOWLEDGEMENTS

I would first like to acknowledge Dr. David Guichet for the premise and development of this project. Without your ingenuity and guidance, this project would not have been possible.

I would like to extend my deepest thanks to my director, Dr. William Nagy. Thank you for your ample readiness to advise and guide me at every turn, and for your capacity for compassion and understanding.

I would also like to acknowledge my committee members, Dr. Elias Kontogiorgos, Dr. Jorge Gonzalez, and Dr. Frank Higginbottom. You have not only assisted me throughout this arduous research project, but also in several other aspects of my journey throughout my residency. Thank you for sharing your time and knowledge.

## CONTRIBUTORS AND FUNDING SOURCES

### **Contributors**

This work was supervised by a thesis committee consisting of Dr. William Nagy, Dr. Elias Kontogiorgos, and Dr. Jorge Gonzalez.

The data analyzed for Section 2.7 was completed in collaboration with Dr. Elias Kontogiorgos.

All other work for the thesis was completed independently by the student.

### **Funding Sources**

Financial support for this project was provided by the American Academy of Fixed Prosthodontics in the form of a research grant. In addition, financial support was provided by Texas A&M in the form of a research grant.

# TABLE OF CONTENTS

	Page
ABSTRACT.....	ii
DEDICATION.....	iv
ACKNOWLEDGEMENTS.....	v
CONTRIBUTORS AND FUNCTION SOURCES .....	vi
TABLE OF CONTENTS .....	vii
LIST OF FIGURES .....	viii
1. INTRODUCTION AND LITERATURE REVIEW .....	1
2. MATERIALS AND METHODS.....	9
2.1 Definitive Cast Fabrication.....	10
2.2 Abutment and Crown Fabrication.....	11
2.2.1 Group 1 –Interrupted Digital Atlantis Workflow .....	11
2.2.2 Group 2 – Full Digital Atlantis Workflow.....	17
2.2.3 Group 3 – Full Digital Split-File Workflow .....	19
2.3 Abutment and Crown Preparation for Measurement.....	23
2.4 Geomagic Measurements.....	24
2.5 SEM Measurements .....	30
2.6 Geomagic Validation .....	33
2.7 Statistical Analysis.....	36
3. RESULTS .....	37
4. DISCUSSION .....	42
5. CONCLUSIONS .....	49
REFERENCES .....	50

## LIST OF FIGURES

	Page
Figure 1: Custom Impression Coping Transfer With Digital Workflow .....	3
Figure 2: Marginal Gap.....	8
Figure 3: Marginal Opening.....	8
Figure 4: Patient Model Cast with Custom Impression Post .....	10
Figure 5: Group 1, Interrupted Digital Atlantis Workflow .....	11
Figure 6: Atlantis Scan Body .....	11
Figure 7: Definitive Cast with Atlantis Scan Body .....	12
Figure 8: Definitive Cast with Atlantis Scan Body in Lab Scanner .....	12
Figure 9: Digitized Definitive Cast with Atlantis Scan Body.....	13
Figure 10: Atlantis Web Editor.....	13
Figure 11: Atlantis Abutment .....	14
Figure 12: Atlantis Abutment in Definitive Cast.....	15
Figure 13: Atlantis Abutment in Definitive Cast in Lab Scanner.....	15
Figure 14: Group 1, Digital Crown Design with Abutment Visualization.....	16
Figure 15: Group 1, Digital Crown Design .....	16
Figure 16: Group's 2 and 3 Full Digital Workflow.....	17
Figure 17: Group 2 Atlantis Core File Abutment Imported into .....	18
Figure 18: Group 2 Digital Crown Design .....	18
Figure 19: Biodenta Scan Body .....	19
Figure 20: Biodenta Scan Body in Definitive Cast.....	19

Figure 21: Group 3 Definitive Cast with Scan Body in Lab Scanner.....	20
Figure 22: Group 3 Digital Abutment Design .....	20
Figure 23: Group 3 Digital Crown Design with Abutment Visualization .....	21
Figure 24: Group 3 Digital Crown Design .....	21
Figure 25: Group 3 Titanium-Base Zirconia Abutment .....	22
Figure 26: Group 3 Zirconia Crown .....	22
Figure 27: Creation of Silicone Replica of Cement Gap .....	26
Figure 28: Geomagic Alignment and Measuring Protocol .....	28
Figure 29: Sectioned Specimen with Measurement Locations. Measurements Taken at Locations A,B,C,H,I,J Were Averaged to Find Average Marginal Gap. Measurements Taken at Locations A,J Were Averaged to Find Average Marginal Opening. ....	32
Figure 30: SEM Mid-Buccal (Fig 29,D) Measurement .....	32
Figure 31: Geomagic Cross-Section .....	34
Figure 32: Geomagic Cross-Section with Measurement Annotations.....	35
Figure 33: 2D SEM Mean Marginal Opening Comparison of 3 Groups.....	37
Figure 34: 2D SEM Mean Marginal Gap VS 3D Geomagic Mean Marginal Gap Comparison of 3 Groups.....	39
Figure 35: 3D Geomagic Mean Internal Fit Comparison of 3 Groups .....	39
Figure 36: 2D Geomagic (GM) Point Measurement VS 2D SEM Point Measurement..	40
Figure 37: First Geomagic Measurement (Run_1) VS Second Geomagic Measurement (Run_2) for Geomagic Repeatability Comparison .....	41
Figure 38: Geomagic 3D & 2D Analysis of Each Group .....	46

## LIST OF TABLES

	Page
Table 1: Mean 2D SEM Marginal Opening of 3 Experimental Groups .....	37
Table 2: Mean 2D SEM Marginal Gap of 3 Experimental Groups .....	38
Table 3: Mean 3D Geomagic Marginal Gap of 3 Experimental Groups .....	38
Table 4: Mean 3D Geomagic Internal Fit of 3 Experimental Groups .....	40
Table 5: Paired t-test p-values for Comparison of 2D SEM Mean Marginal Gap Compared to 3D Geomagic Mean Marginal Gap .....	41

## 1. INTRODUCTION AND LITERATURE REVIEW

Computer-assisted design (CAD) and computer-assisted manufacturing (CAM) has grown in widespread acceptance and use in implant dentistry. Continuous improvements in CAD/CAM technology accuracy has challenged conventional techniques for prostheses and abutment fabrication.<sup>1-4</sup> In a recent systematic review Kapos and Evans<sup>1</sup> concluded that implant abutment and crown CAD/CAM technology is able to provide results that are comparable to that of conventional techniques in terms of implant survival, prosthesis survival, technical and biological complications. In addition, digital workflows can be more time-efficient, reducing clinical chair time and laboratory manufacturing steps.<sup>5</sup>

There are several workflow approaches for implant-supported restoration fabrication. We are no longer bound to a pure analog methodology. With the advent of CAD/CAM, one has the option to attempt a full digital approach to fabrication, or to integrate advantages of both old and new ways to accomplish ideal results. The path chosen is likely to vary on a case-by-case basis. Workflows will vary based on open versus closed architectures, available software and equipment, and the proprietary nature of implant parts and components. Among other factors to consider are patient time spent in the chair, chair-side time for the dentist, and which approach will yield the most predictable and esthetic outcome.

As full digital workflow technology is still relatively new and precision often questioned, intermediate steps are sometimes taken to insure accuracy. An interjected step into a digital workflow often occurs upon receiving a custom designed and milled

abutment. Once received, the abutment is checked for accuracy with an intra-oral try-in, or by inserting the abutment in the patient's cast. The abutment is then scanned for CAD/CAM crown fabrication. The try-in and re-scan step taken outside of the digital workflow takes additional time for the clinician and patient, introduces additional cost, and potentially creates a deleterious effect on peri-implant tissue.

The soft tissue response around implant-supported restorations is affected by many variables.<sup>6</sup> A generally accepted hypothesis is that repeated disconnection or mechanical disruption of implant components around peri-implant tissue has detrimental effects, including the possibility of apical migration of bone and soft tissue.<sup>6-9</sup> Therefore clinicians should mitigate disconnection effects by decreasing the frequency of mechanical disruption of the peri-implant soft tissue. If desired soft tissue morphology is acquired in the final impression, one could fabricate the custom abutment and the final crown simultaneously, removing the step of trying in the custom abutment, thereby sparing the peri-implant tissue of an additional mechanical disruption.

There are multiple ways to shape peri-implant tissue to create proper emergence for the final crown. Initially, an anatomical healing abutment can be attached immediately after implant placement or after uncovering the implant at a second stage surgery. Once an implant is integrated and the cover screw or healing abutment has been removed, one can choose to shape the peri-implant tissue with a final custom abutment and provisional, or with a provisional and a temporary cylinder. The use of a temporary cylinder and provisional to shape peri-implant tissue, particularly in the esthetic zone, is well documented in the literature. Once the tissue is shaped, one can then utilize any of the



several ways to replicate desired soft tissue morphology and emergence profile when taking a final impression for implant-abutment and crown fabrication.<sup>10, 11</sup> Papadopoulos et al<sup>11</sup> have illustrated four ways to transfer the emergence profile from the provisional to the final restoration. Perhaps the most utilized is the modification of the impression post by adding resin extra-orally. One could utilize this technique to acquire ideal peri-implant morphology into their impression and master cast. Once this cast has been fabricated, the clinician could transfer to a full digital workflow for the remainder of the abutment and crown fabrication process (Figure 1).



**FIGURE 1: CUSTOM IMPRESSION COPING TRANSFER WITH DIGITAL WORKFLOW**

Current CAD/CAM technology allows clinicians to fully customize abutments to match clinical situations.<sup>1, 4, 12</sup> A scan body is inserted intra-orally or into the patient's master cast and an intra-oral scanner or lab scanner is used to transfer the implant location within the dental arch to design software. Some dental software programs permit operators the option to design an abutment and immediately proceed to crown design and fabrication. An abutment can be designed, and an .STL (Standard Tessellation Language) file of that abutment can be used to design a crown.

Customized titanium Atlantis (Dentsply, Molndal, Sweden) abutments have been shown to be clinically acceptable.<sup>13</sup> When ordering an Atlantis abutment, an initial design is created based on prescription selections. Once completed this digital design can be viewed and altered through an editor on the Atlantis web interface. Upon ordering, there is an option to receive an .STL of the designed abutment. The Atlantis .STL, called an Atlantis Core File, is a digital representation of the outer surface of the abutment and its surrounding that enables the design of the coping and final restoration even before receiving the physical Atlantis abutment order.<sup>14</sup> The Core File can be imported into design software and used to proceed with crown design and milling. The customized Atlantis abutment and milled crown can then be delivered to the patient in one appointment.

In some cases, zirconia abutments offer a good alternative to titanium abutments. Yttria-stabilized tetragonal zirconia is a common material used for various dental applications including fixed dental prostheses, crowns and implant abutments.<sup>15-19</sup> Zirconia is considered to be more biocompatible than titanium, other metal alloys and ceramics, and therefore may result in a superior peri-implant soft tissue response.<sup>17, 19-23</sup> In addition, zirconia can be an advantage due to its' toughness and esthetic advantages over other materials.<sup>24-27</sup> Two-piece abutments with a titanium base cemented into a zirconia abutment have been shown to be more successful than one-piece zirconia abutments.<sup>28</sup> These offer a more reliable alternative to one-piece zirconia abutments in esthetically demanding cases where zirconia is preferred over titanium.

Research has shown all-ceramic CAD/CAM restorations provide superior color

matching and clinically acceptable outcomes.<sup>1</sup> It has been shown that better fit can be achieved with CAD/CAM zirconia compared to conventional metal-ceramic fabrication.<sup>29</sup> After design, CAD/CAM abutments and crowns can be milled by outside lab milling units or in-office milling units. There is a wide array of milling units now available based on what materials they mill, as well as their complexity and accuracy. Some milling units have been shown to provide greater accuracy than others. Bosch et al<sup>30</sup> evaluated 5-axial and 4-axial milling units, and found that the 5-axial milling unit they evaluated produced restorations with fewer deviations from their digital designs than 4-axial milling units. The Atlantis mill is an example of a 5-axis mill. Another example of a 5-axis mill is the Zirkonzahn (Zirkonzahn GmbH, Bruneck, Italy) M1 milling unit, a 5+1 axes simultaneous milling unit with 1 milling spindle. The M1 can mill several materials, including yttria-stabilized tetragonal zirconia, which can be used for both abutment and crown material. Lins et al<sup>31</sup> studied three different milling units for the fit of zirconia copings on anatomical titanium abutments, and found all three to have acceptable marginal fit. Ha and Cho<sup>32</sup> discovered monolithic zirconia crowns and porcelain-fused zirconia coping crowns manufactured with Zirkonzahn systems are acceptable for clinical settings. Sheridan et al<sup>33</sup> found acceptable fit of zirconia crowns to zirconia abutments, both fabricated from a full digital split-file workflow.

With the advent of two-piece titanium-base abutments, the customized portion of the abutment can be milled in-office from zirconia. The same milling unit can be used to mill zirconia crowns. This presents the potential for an in-office full digital workflow. 3Shape (3Shape Dental System, 2016, Denmark) software offers the split-file workflow

which facilitates abutment and crown design simultaneously from one initial scan of the implant location.<sup>33-35</sup> The crown and abutment can then be milled, and without try-in or re-scan be delivered to the patient in a single visit. Sheridan et al<sup>33</sup> evaluated the split-file workflow against several more conventional interrupted workflows, and found that after adjustments, the complete digital workflow produced clinically acceptable results.

Inadequate fit and adaptation of crowns to their abutments can lead to mechanical complications such as marginal chipping or veneering fracture, which could later lead to clinical failure.<sup>36, 37</sup> Excessive cement space has been shown to influence failure of the veneering porcelain.<sup>37</sup> An open margin could serve as a bacterial nidus, leading to gingival inflammation.<sup>38-40</sup> In addition, open margins can be a disadvantage as they may lead to disintegration of the cement layer.<sup>40, 41</sup>

There are several methods to measure marginal gap. Holmes et al<sup>42</sup> first described internal and marginal gap measurements and Sorensen<sup>43</sup> described several other methods. Many studies have defined their marginal gap measurements by just the vertical, or vertical and horizontal measurement between the restoration and the die at the marginal opening<sup>32, 42, 44, 45</sup>. Groten et al<sup>46</sup> determined that a minimum of fifty measurements are required to determine marginal gap. With the advent of digital measuring procedures, we have the capabilities of measuring at several locations, including three-dimensional measurements as opposed to two-dimensional measurements traditionally reported in the literature. Digital measuring procedures have been used to measure marginal gap by evaluating the fit of the crown to the die over the entire surface of the die or abutment margin.<sup>47, 48</sup> The entire internal fit has also been calculated with digital measuring

techniques.<sup>2, 49-52</sup> Various studies have indicated a suggested marginal gap of 120 µm or less is required for high probability of clinical success for ceramic restorations.<sup>53, 54</sup> However, there is no consensus on acceptable marginal opening for all ceramic crowns on implant abutments. Martinez-Rus et al<sup>55</sup> used 120µm as the acceptable marginal opening for ceramic crowns on abutments based on findings in previous studies.<sup>54</sup>

The purpose of this study was to evaluate two full digital workflows by measuring internal fit, marginal gap and marginal opening of a CAD/CAM crown and abutment designed from one initial scan, compared to the more customary interrupted workflow that includes a secondary scan of the custom abutment prior to final crown design and fabrication. For the purposes of this study the crown adaptation to the abutment was evaluated with three different measurements. First, internal fit of the entire crown intaglio was evaluated with engineering software, and one final average measurement was recorded. Second, the entire preparation margin was evaluated with engineering software and one average marginal gap was recorded (Figure 2). In addition, measurements were acquired with Scanning Electron Microscope (SEM) along the preparation margin of the abutment and were averaged to find an average marginal gap. Third, vertical measurements from the crown intaglio to abutment surface at the outer most aspect of the margin were taken on each specimen with SEM, and averaged to find an average marginal opening (Figure 3). Engineering software was used to evaluate internal fit and marginal gap, and Scanning Electron Microscopy (SEM) was used for marginal gap, marginal opening, and software validation. Recorded marginal gap measurements were then compared to the standard 120µm to determine clinical acceptability and relevance. The

null hypothesis was there would be no difference in internal fit, marginal gap and marginal opening between the three groups.

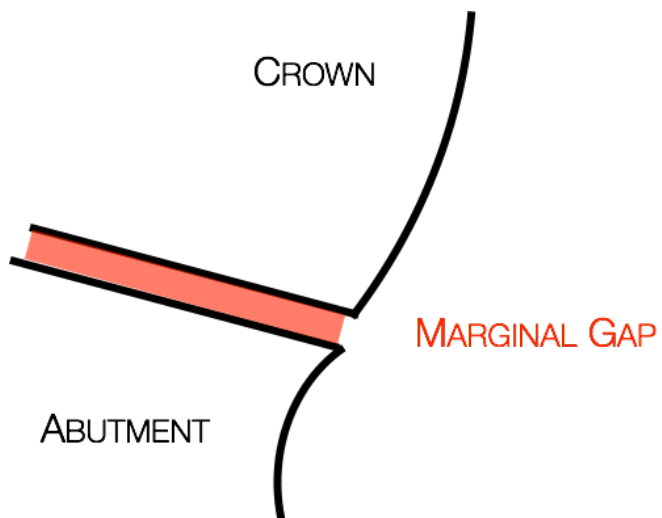


***FIGURE 2: MARGINAL GAP***

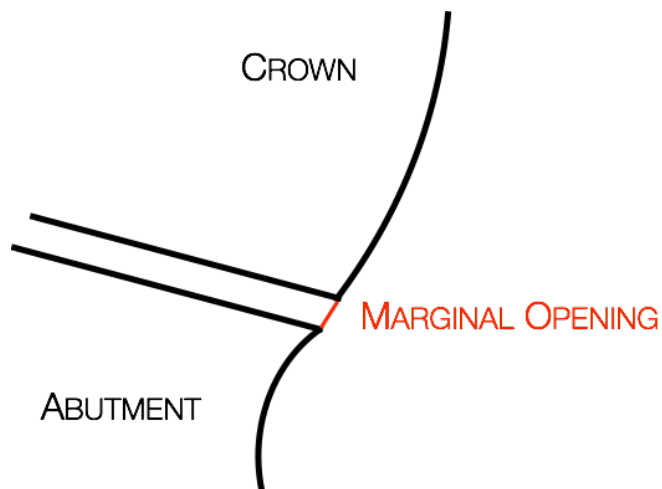


***FIGURE 3: MARGINAL OPENING***

## 2. MATERIALS AND METHODS

Three different workflows were designed and compared. Group 1, “Interrupted Digital Atlantis Workflow”, represented the most utilized customary workflow, which included a customized Atlantis abutment that was designed and received, and then re-scanned for final crown design. Group 2, “Full Digital Atlantis Workflow”, included a customized Atlantis abutment and its corresponding .STL, the Atlantis Core File, which was immediately imported into design software and used for crown design and milling. Group 3, “Full Digital Split-File Workflow”, utilized 3Shape’s full digital workflow for abutment and crown design called the split-file workflow. This included a titanium-base zirconia abutment and zirconia crown that was designed concurrently and then milled simultaneously. Titanium-base zirconia abutments were composed of titanium bases provided by Biodenta (Biodenta Hybrid Ti-Base, Switzerland) and zirconia abutments milled with a 5-axis mill (Zirkonzahn M1, GmbH, Bruneck, Italy), from zirconia blocks (Zirkonzahn Translucent, GmbH, Bruneck, Italy). Atlantis titanium abutments were milled by Atlantis with their 5-axis mill.

All crowns were designed using 3Shape’s default settings for Zirconia copings with the following settings: “0.025mm” cement gap and an “0.040mm” extra cement gap with “1.00mm” distance to margin line. The crown thickness was greater than 1 mm. Margins were milled with extra horizontal width per default settings of the software to mitigate risk of chipping during the milling process. All crowns were milled with a 5-axis mill (Zirkonzahn M1), using green-stage zirconia (Prettau, Zirkonzahn GmbH), then sintered according to manufacturer specifications.

## 2.1 Definitive Cast Fabrication

A single definitive cast was fabricated with an implant analog in tooth number five position from a final impression with a custom impression post with desired emergence profile of the soft tissue (Figure 4). Astra Tech EV (Dentsply, Molndal, Sweden) conical 4.2x11 implant and its' corresponding analog were used. Scans were acquired with a lab scanner (3Shape D900, 3Shape, Denmark). Precision of the D900 is 8 microns.

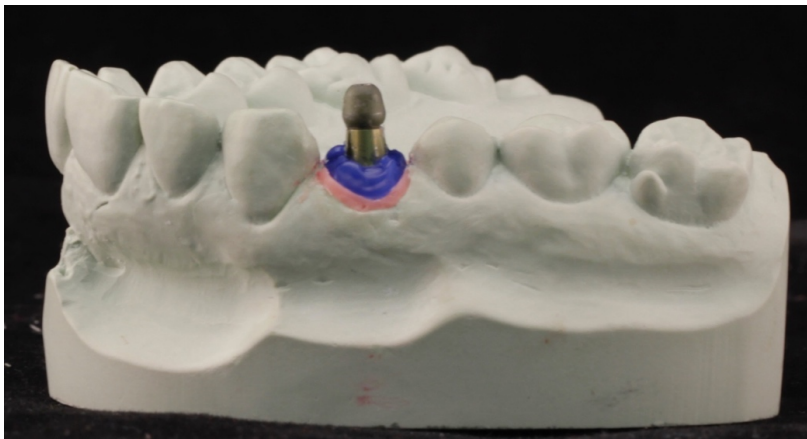


***FIGURE 4: PATIENT MODEL CAST WITH CUSTOM IMPRESSION POST***



## 2.2 Abutment and Crown Fabrication

### 2.2.1 Group 1 –Interrupted Digital Atlantis Workflow

For Group 1, the digital workflow of fabrication and acquisition of a CAD/CAM custom abutment and crown was interrupted by scanning the abutment once received from Atlantis (Figure 5).

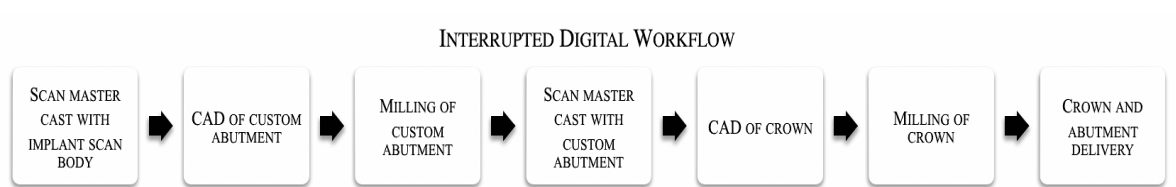


**FIGURE 5: GROUP 1, INTERRUPTED DIGITAL ATLANTIS WORKFLOW**

An implant scan body (Atlantis, Dentsply, Molndal, Sweden) was secured into the definitive cast implant analog and digitized with the lab scanner (Figures 6-9).



**FIGURE 6: ATLANTIS SCAN BODY**

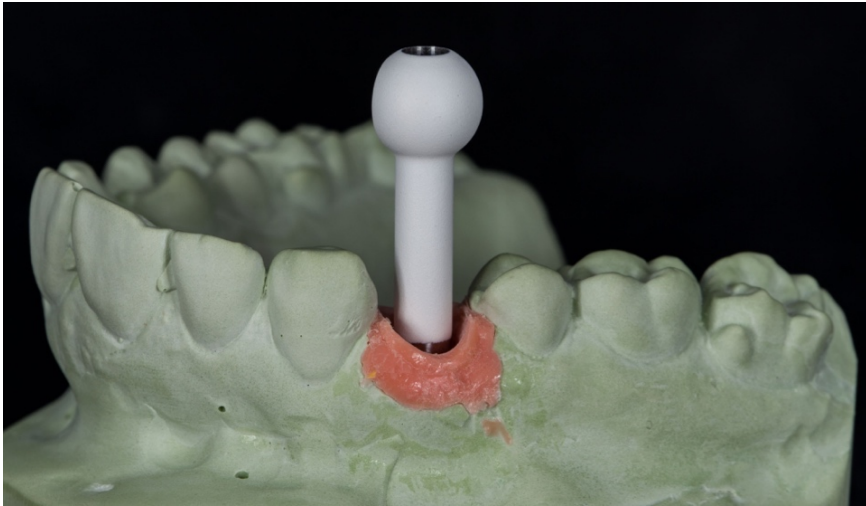


***FIGURE 7: DEFINITIVE CAST WITH ATLANTIS SCAN BODY***

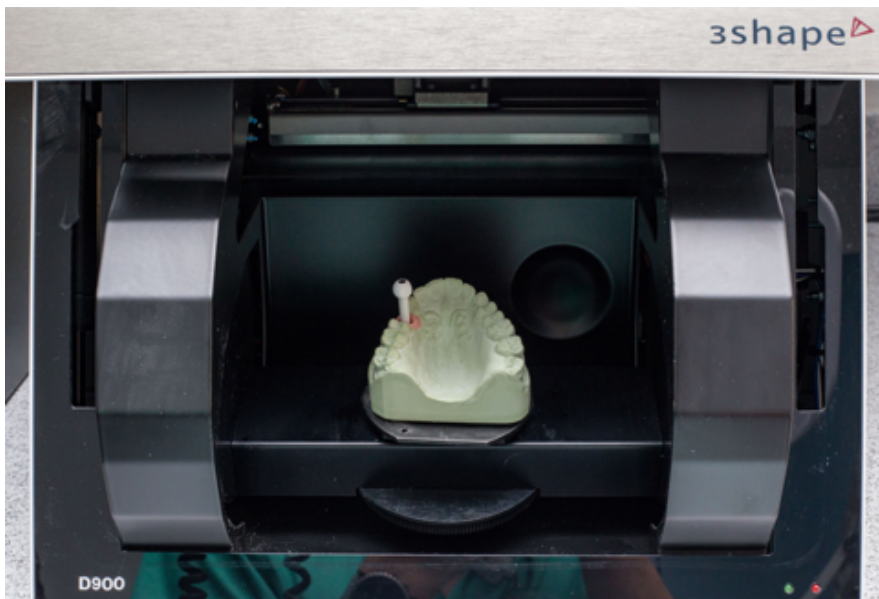


***FIGURE 8: DEFINITIVE CAST WITH ATLANTIS SCAN BODY IN LAB SCANNER***

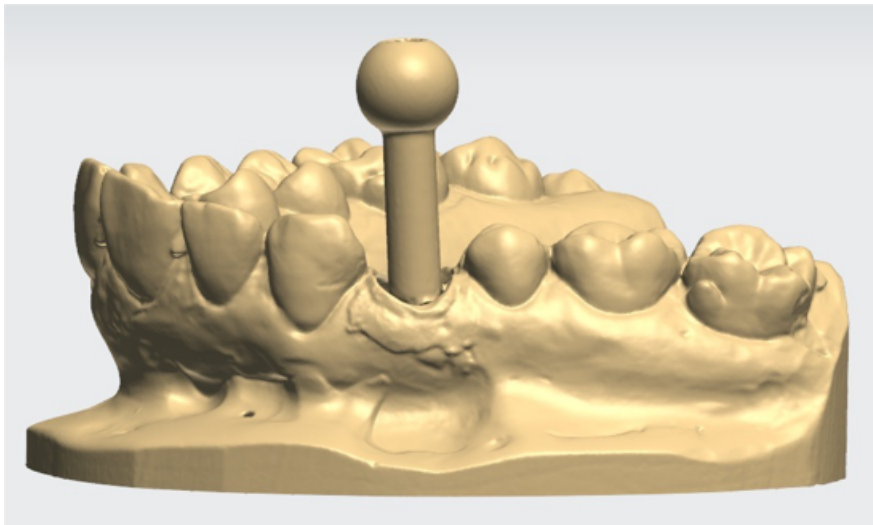


**FIGURE 9: DIGITIZED DEFINITIVE CAST WITH ATLANTIS SCAN BODY**

An .STL of the cast was sent to Atlantis for custom abutment fabrication. The abutment was designed and customized through the Atlantis web interface editor, and fourteen abutments of the single design were requested (Figure 10,11).

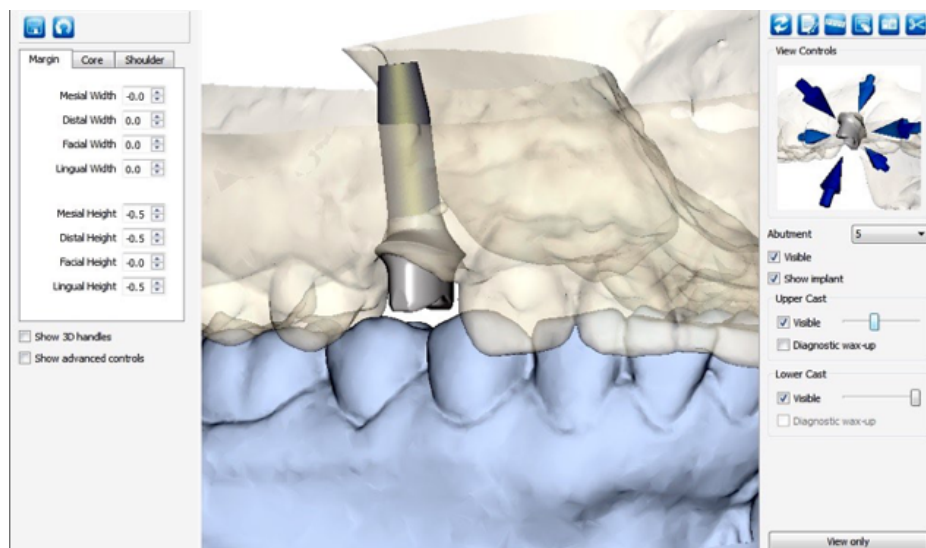


**FIGURE 10: ATLANTIS WEB EDITOR**



***FIGURE 11: ATLANTIS ABUTMENT***

Half (seven) of the requested abutments were used for Group 1, and the other half (seven) were used for Group 2. Once the seven abutments for Group 1 were received, they were placed in the definitive cast, and individually re-scanned for crown design and fabrication (Figure 12,13). One zirconia crown with a facial cutback was designed for each of the seven abutments, then sent for milling (Figure 14,15).

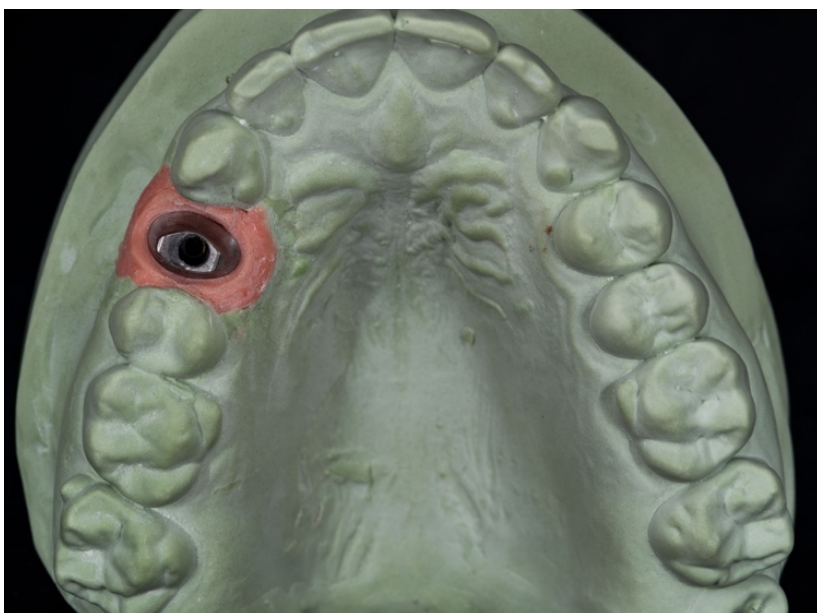


***FIGURE 12: ATLANTIS ABUTMENT IN DEFINITIVE CAST***

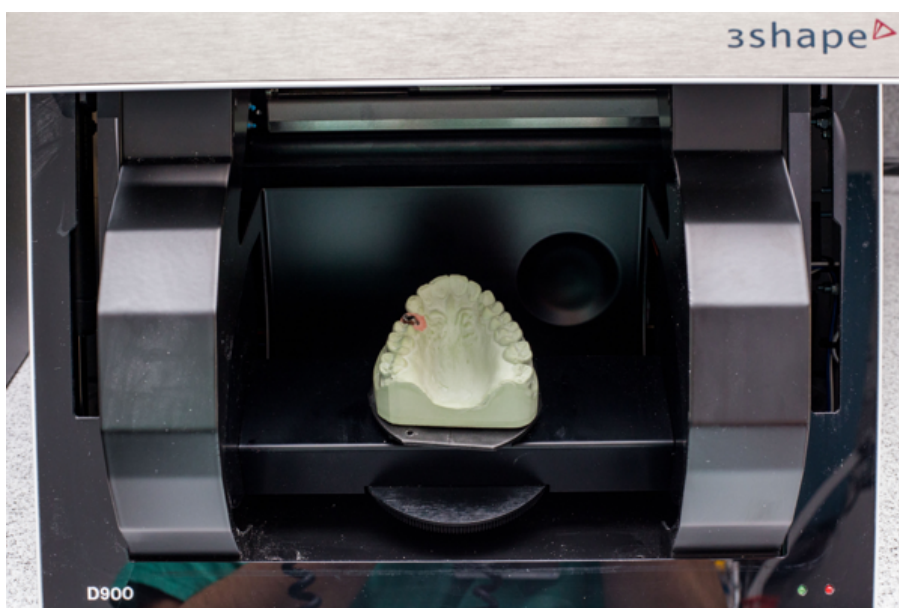


***FIGURE 13: ATLANTIS ABUTMENT IN DEFINITIVE CAST IN LAB SCANNER***



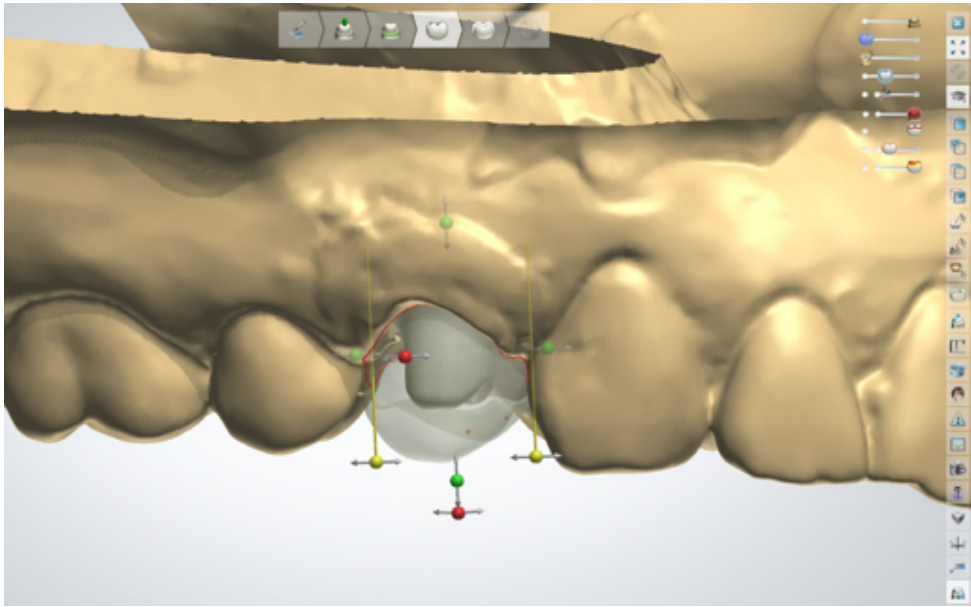


***FIGURE 14: GROUP 1, DIGITAL CROWN DESIGN WITH ABUTMENT VISUALIZATION***

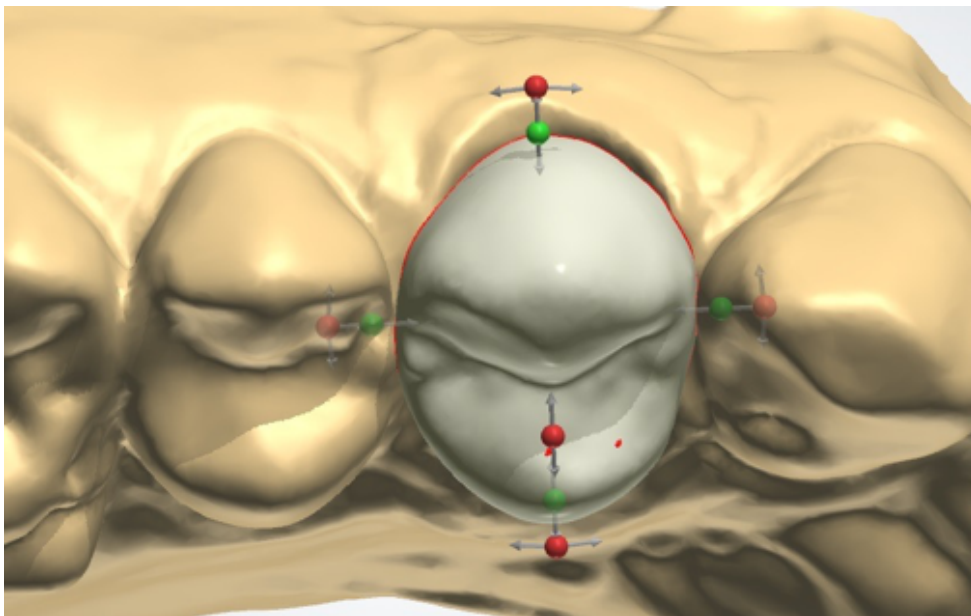


***FIGURE 15: GROUP 1, DIGITAL CROWN DESIGN***

### 2.2.2 Group 2 – Full Digital Atlantis Workflow

Group 2 was carried out with custom abutment and crown fabrication using a full digital workflow (Figure 16). As previously described, after scanning the cast and implant scan body, the .STL of the implant in the definitive cast was sent to Atlantis for custom abutment fabrication. The abutment was customized through the web interface and fourteen abutments of the single design were requested (Figure 10). Once the abutment design had been finalized, the Atlantis Core File, an .STL of the customized Atlantis abutment was imported into 3Shape design software, allowing for immediate crown design (Figure 17). A custom zirconia crown was then designed (Figure 18). Once design was complete, the exported crown STL was sent to the milling unit and seven zirconia crowns were milled from the single STL design, before the final seven abutments had physically been received from Atlantis.



***FIGURE 16: GROUP'S 2 AND 3 FULL DIGITAL WORKFLOW***

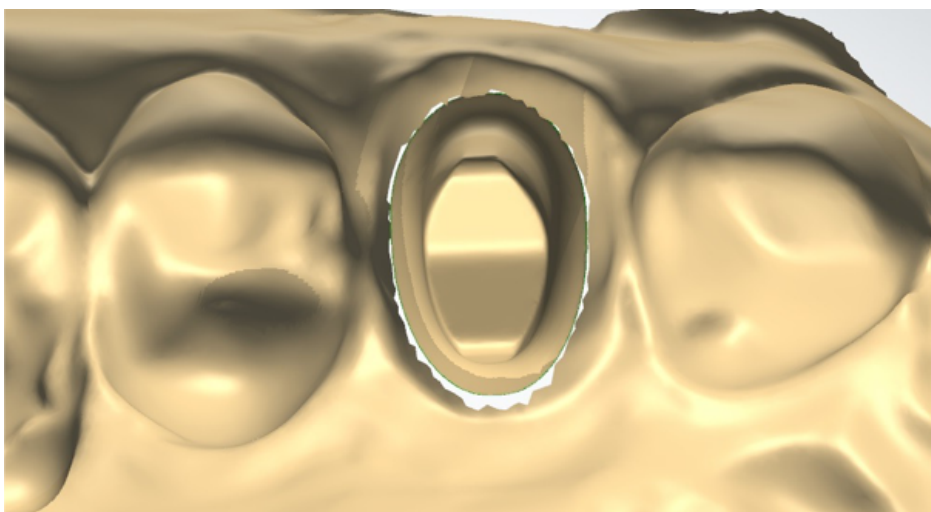


***FIGURE 17: GROUP 2 ATLANTIS CORE FILE ABUTMENT IMPORTED INTO 3SHAPE DESIGN SOFTWARE***

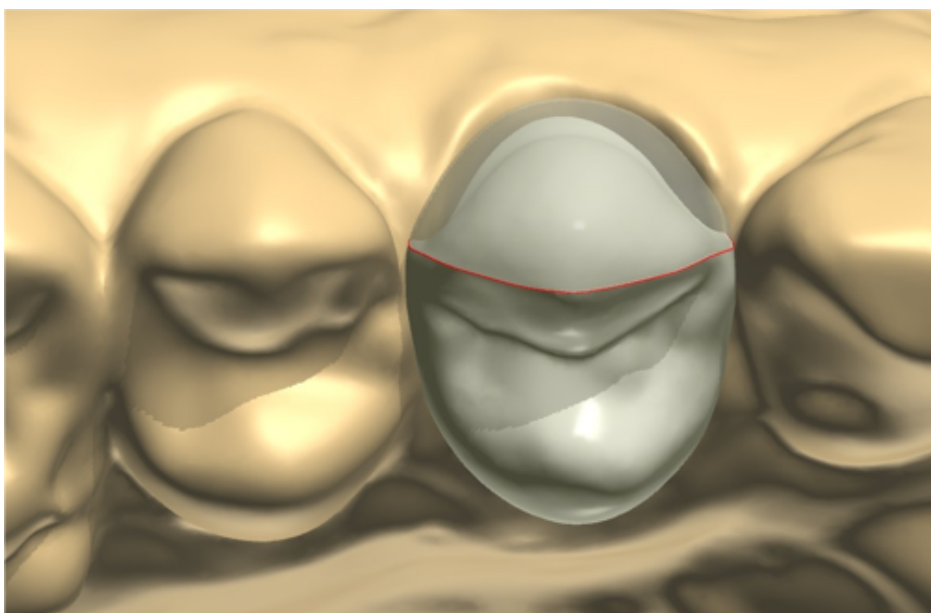


***FIGURE 18: GROUP 2 DIGITAL CROWN DESIGN***



### 2.2.3 Group 3 – Full Digital Split-File Workflow

Group 3 also used a full digital workflow for custom abutment and crown fabrication (Figure 16). For Group 3, a Biodenta scan body was placed in the definitive cast and scanned using 3Shape D900 (Figure 19,20,21).

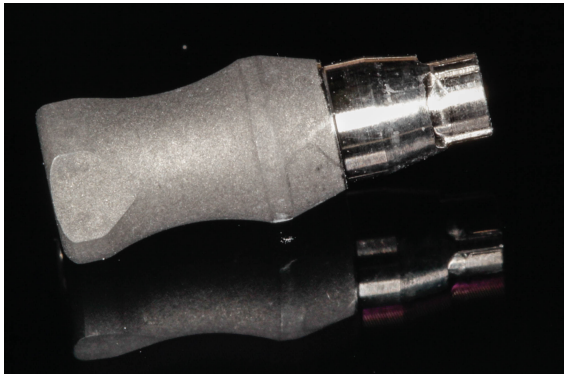


***FIGURE 19: BIODENTA SCAN BODY***

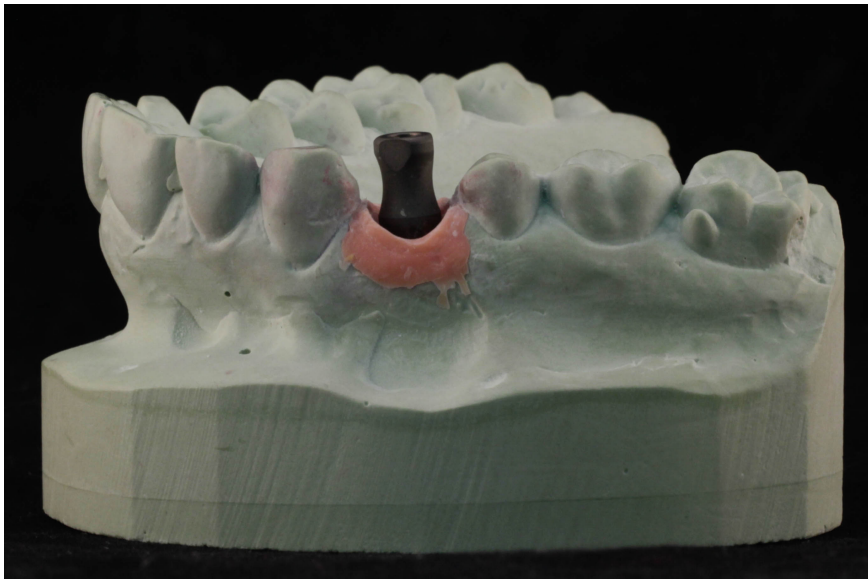


***FIGURE 20: BIODENTA SCAN BODY IN DEFINITIVE CAST***

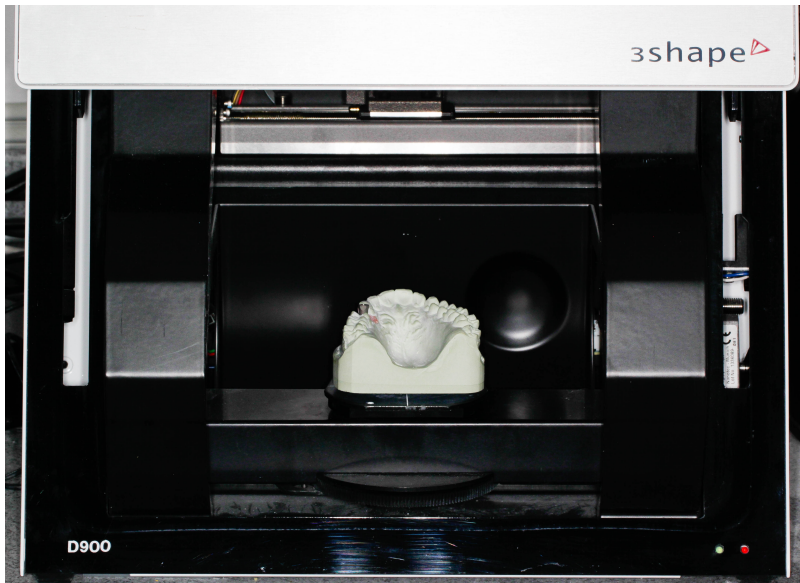


***FIGURE 21: GROUP 3 DEFINITIVE CAST WITH SCAN BODY IN LAB SCANNER***

3Shape's Split-File work-flow was utilized, in which the zirconia abutment and crown were designed consecutively from the single scan (Figure 22,23,24).<sup>34</sup> Once designed the zirconia abutment and zirconia crown were exported as STL's and sent to the milling unit. From the single STL files, seven zirconia abutments and crowns were milled (Figure 25,26).

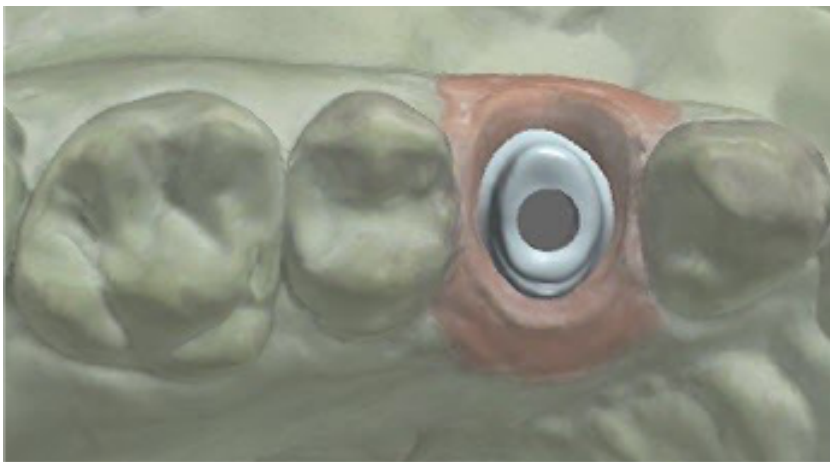


***FIGURE 22: GROUP 3 DIGITAL ABUTMENT DESIGN***

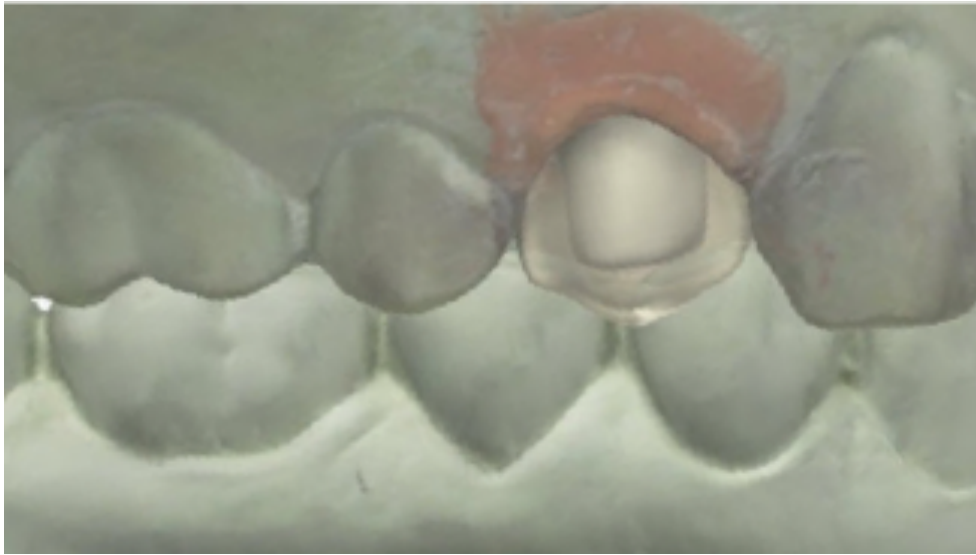


***FIGURE 23: GROUP 3 DIGITAL CROWN DESIGN WITH ABUTMENT VISUALIZATION***

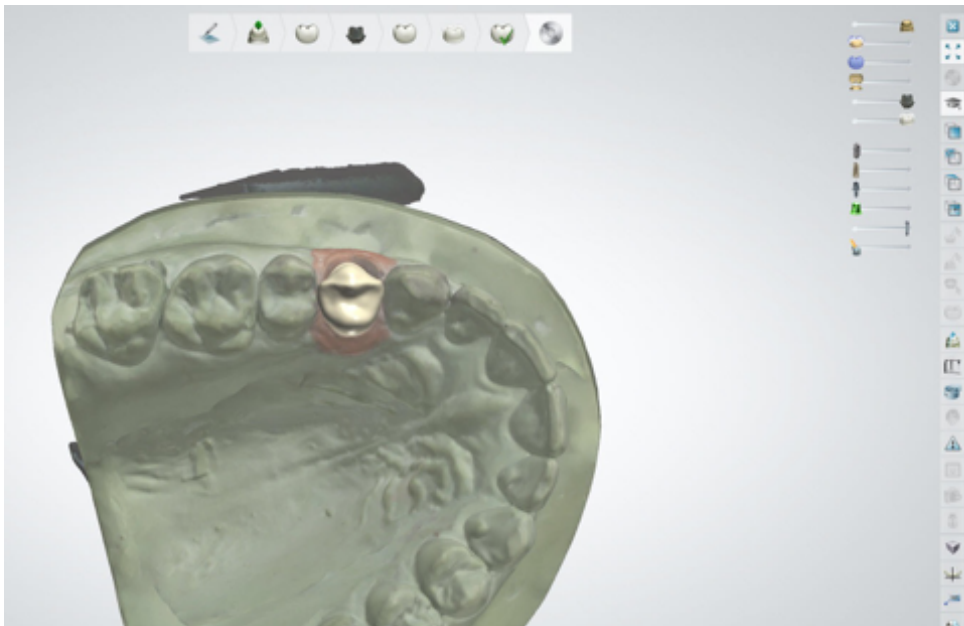


***FIGURE 24: GROUP 3 DIGITAL CROWN DESIGN***



***FIGURE 25: GROUP 3 TITANIUM-BASE ZIRCONIA ABUTMENT***



***FIGURE 26: GROUP 3 ZIRCONIA CROWN***

### 2.3 Abutment and Crown Preparation for Measurement

Two forms of measurement were used for the purposes of this study. Specimens were first prepped and analyzed with Geomagic (Geomagic Control 2015; 3D Systems) software using a new modified technique. Geomagic software allowed for three-dimensional measurements of internal fit and marginal gap with thousands of measuring points per specimen. Next, crowns were cemented, embedded and sectioned, and measured with a Scanning Electron Microscope (SEM) for two-dimensional measurements at twelve standardized locations per specimen.

## 2.4 Geomagic Measurements

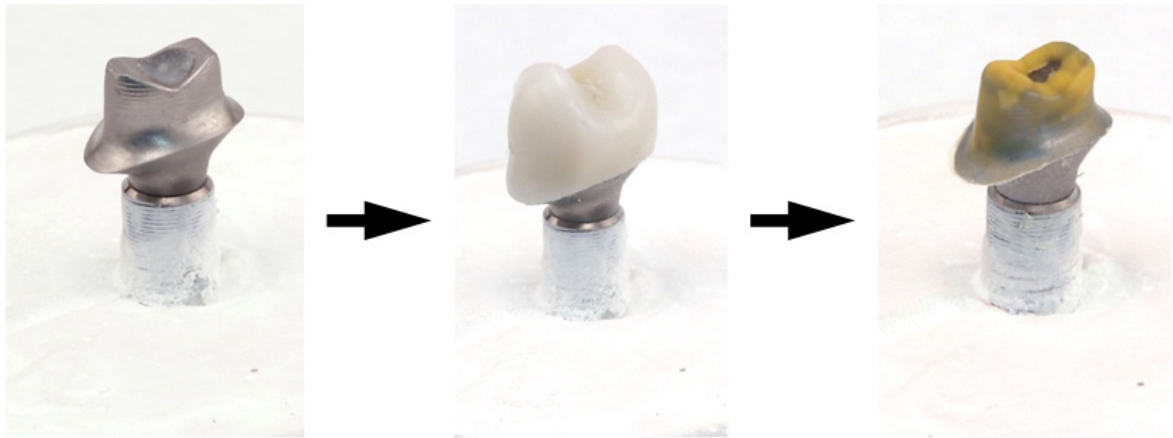
Engineering software has been used for several purposes within the dental literature.<sup>2, 47, 48, 50-52, 56-60</sup> Stephan Holst used engineering software to develop the triple scan protocol to be used to digitally measure and evaluate internal fit and marginal gap.<sup>48, 52</sup> Another form of measurement of internal fit and marginal gap is the silicone replica technique, which has been validated in the literature.<sup>61-67</sup> For this technique, polyvinyl siloxane (PVS) impression material is used to replicate the internal space between a die and crown, and then evaluated to assess internal fit and marginal gap.

A digital measuring technique has been established with a PVS replica of the internal space, whereby a die is first scanned, then the same die with a silicone replica fixated on the die is scanned, and the two scans are digitally over-layed and then used to measure internal fit.<sup>2, 50, 51, 58, 59</sup> In a similar technique, a PVS replica has been used as a means to evaluate internal fit using Geomagic software.<sup>68</sup> For this study, previous methods have been used and modified, then validated with SEM measurements. Geomagic measurements were taken for all three groups in the same standardized way prior to final crown cementation and SEM analysis.

First, specimens were prepped for measuring by creating a silicone replica of the cement space on the abutment (Figure 27). A base was fabricated securing the AstraTech EV conical 4.2x11 implant into stone. The stone base included distinguishing marks that could later be used within the software as markers to overlay scans. Prior to securing the abutment, the area below the finishing line of the abutment was lightly air-abraded to reduce reflectivity and need for a coating spray on the base between scans. Next, the

abutment was secured to the base by tightening the abutment screw. The abutment surface above the finishing line was then coated with a light spray to reduce reflectivity, then scanned with the 3Shape D900 lab scanner. Once scanning was completed, the abutment and the abutment's corresponding crown were both cleaned with alcohol then dried. The abutment was then coated with a very thin layer of PVS adhesive, then allowed to dry. Next, the crown was filled with light body PVS, then seated onto the secured abutment with firm finger pressure as the excess PVS was quickly removed. The crown-abutment unit was then placed under 5lbs of standardized pressure for ten minutes. Once setting was complete, the crown was quickly removed from the abutment, leaving the internal space PVS-replica firmly adhered to the abutment. The PVS-coated abutment was then scanned with the D900 lab scanner.

GROUP 2 ATLANTIS ABUTMENT, CROWN, AND SILICONE REPLICA



GROUP 3 Ti-BASE ZIRCONIA ABUTMENT, CROWN, AND SILICONE REPLICA

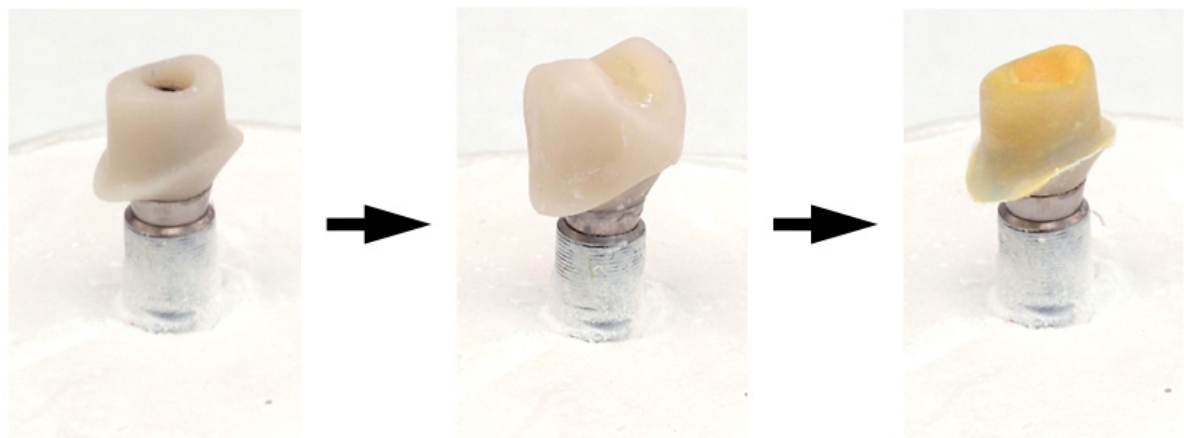


***FIGURE 27: CREATION OF SILICONE REPLICA OF CEMENT GAP***



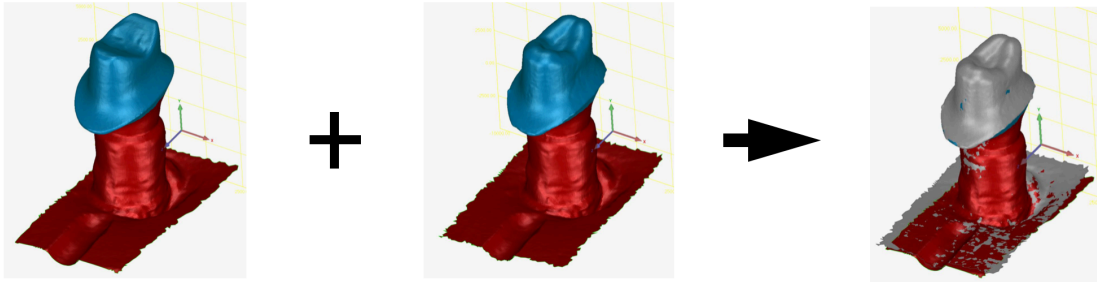
Both the initial abutment scan, and PVS-abutment scan were exported as .STL's and imported into Geomagic software (Figure 28, Step 1). The bases were then virtually trimmed and matched, then highlighted for alignment. When overlaying the two scans, only the base and the emergence portion of the abutment were highlighted, as this was the matching area of both scans. The highlighted areas were first aligned manually through "N-Point Alignment" in which three or more locations were chosen on both scans then aligned accordingly. Following N-Point Alignment, the initial overlay was perfected using the "Best-Fit Alignment" function, checking "High Precision Fitting" and "Fine Adjustments Only" to further correctly align the two scans (Figure 28, Step 2). Once aligned, the alignment was assessed by evaluating a 3D analysis of the selected aligned area. An alignment was considered successful if the deviation between the two scans was a positive average of 6 microns or less, and an RMS estimate of 12 microns or less. These successful alignment values were determined based on a pilot study.

Once the scans were successfully aligned, the bases and anything below the finishing line on the abutments of both scans were deleted, leaving only the abutment and the abutment-PVS of corresponding scans remaining. The abutment-PVS unit was then converted to a point cloud to increase the number of data points utilized for measuring. The entire PVS portion was highlighted, then converted to a point cloud of 200,000 points (Figure 28, Step 3).

STEP 1 - IMPORT STL'S INTO GEOMAGIC



STEP 2 - SELECT BASES AND PREFORM ALIGNMENT



STEP 3 - CREATE POINT CLOUD OF PVS-ABUT AND PREFORM 3D ANALYSES OF CROWN AND MARGIN

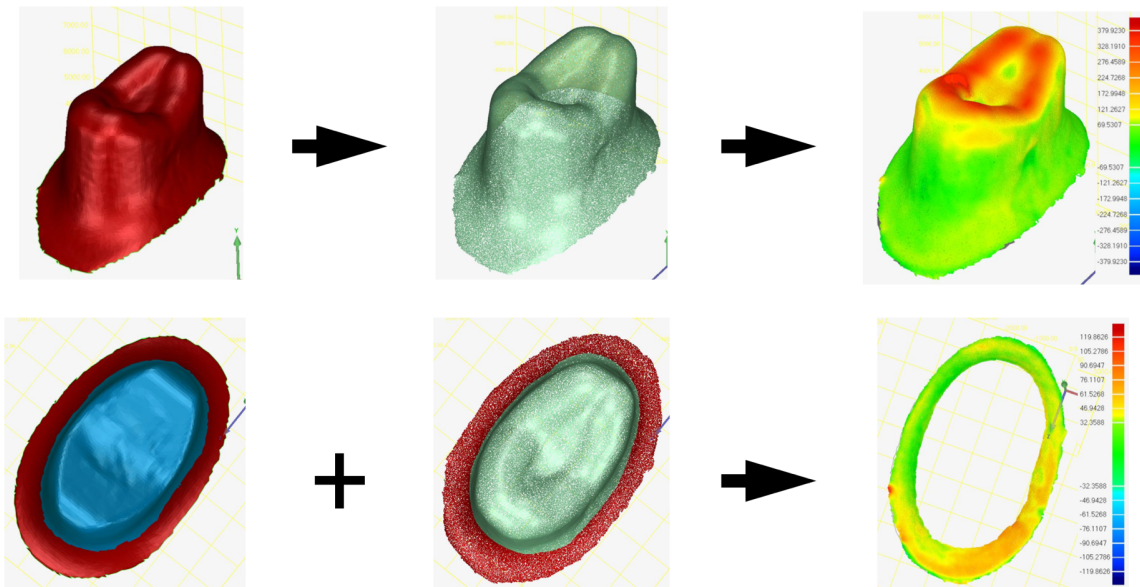


**FIGURE 28: GEOMAGIC ALIGNMENT AND MEASURING PROTOCOL**

Two major measurements were taken with the Geomagic software. First, a 3D analysis was administered to assess the distance between the surface of the reference abutment to the point-cloud of the abut-PVS surface, thereby measuring the crowns' cement space and internal fit (Figure 28, Step 3). For each specimen the average positive deviation of the internal fit was recorded. The deviation was averaged from nearly 197,000 data points. Next, the margins were highlighted on the reference abutment and PVS-abutment point cloud and a 3D analysis was completed to assess the marginal gap (Figure 28, Step 3). Average positive deviation of the marginal gap was recorded. For each marginal gap measurement nearly 57,000 data points were used.

## 2.5 SEM Measurements

The use of Scanning Electron Microscopy (SEM) for the analysis of internal fit is common in the literature.<sup>33, 69, 70</sup> Once scans were completed for Geomagic measurements, abutments and crowns were cleaned and dried. Abutment screw access holes were then filled with PVS and allowed to set. Abutments were then seated in a secure base, and their corresponding crowns cemented (Rely-X Luting Cement, 3M, St. Paul, Minnesota), using standardized pressure of 5lbs for ten minutes. After being allowed to set for twenty-four hours, specimens were embedded, then later sectioned along the long axis in a buccal-lingual direction with a low speed, water-cooled diamond sectioning saw (Buehler Isomet Low-speed Saw; Lake Bluff, Illinois).

The sectioned units for all three groups were placed under an SEM microscope (JEOL 6010LA, JEOL Inc., Tokyo, Japan), and measurements were recorded. Twelve measurements were taken per specimen, two mid-axially both buccal (Figure 29, D) (Figure 30) and palatal (Figure 29, G), and two at the cusp height of contour both buccal (Figure 29, E) and palatal (Figure 29, F). Six measurements were taken at the margin, one at the buccal marginal opening (Figure 29, A), one at buccal mid-margin (Figure 29, B), one at the buccal margin-axial wall junction (Figure 29, C), one at the palatal margin-axial wall junction (Figure 29, H), one at the palatal mid-margin (Figure 29, I), and one at the palatal marginal opening (Figure 29, J).

Overextended or horizontal marginal discrepancy was not measured for the purposes of this study. Mid-axial and cusp height of contour measurements (Figure 29 D,E,F,G) of each specimen were used to compare with Geomagic measurements for

validation purposes. Marginal gap was obtained by averaging all six measurements at the margin of each specimen (Figure 29 A,B,C,H,I,J). Average marginal gap measurements were then used for statistical analyses. Marginal opening was obtained by averaging the outermost marginal measurements (Figure 29 A,J). The marginal opening averages were then used for statistical analyses.

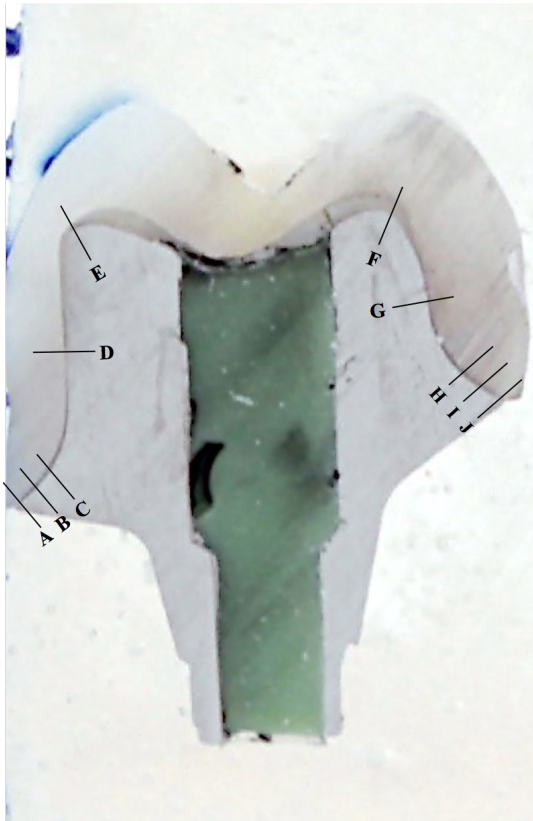


**FIGURE 29: SECTIONED SPECIMEN WITH MEASUREMENT LOCATIONS. MEASUREMENTS TAKEN AT LOCATIONS A,B,C,H,I,J WERE AVERAGED TO FIND AVERAGE MARGINAL GAP. MEASUREMENTS TAKEN AT LOCATIONS A,J WERE AVERAGED TO FIND AVERAGE MARGINAL OPENING.**

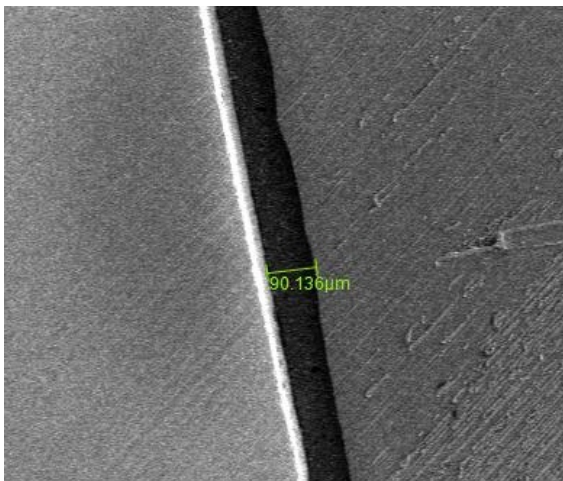


**FIGURE 30: SEM MID-BUCCAL (FIG 29,D) MEASUREMENT**

## 2.6 Geomagic Validation

Due to the novel methodology of the Geomagic measuring protocol, a very thorough validation process took place. First, a 2D analysis was performed with the Geomagic software and was then used to compare to 2D SEM measurements. In order to accomplish this, a digital cross-section was made through the 3D aligned abutment/abutment-PVS unit at approximately the same location as the buccal-lingual section of the corresponding SEM specimen, resulting in a 2D cross-section (Figure 31,32). 2D Geomagic measurements were taken at the same locations as the 2D SEM sectioned specimens. Using samples from each group, a total of fifty measurements were recorded, twenty-five from 2D Geomagic and twenty-five of the same location of the same specimens from 2D SEM (Figure 32). The fifty measurements were then statistically compared.

In addition, for each SEM section, the six marginal measurements recorded per specimen were averaged to find average marginal gap. Then marginal gap averages of 3D Geomagic measurements were statistically compared with marginal gap averages found with 2D SEM measurements.

Last, to insure repeatability of the new Geomagic measuring technique, alignment and analysis was repeated on samples from each group, totaling eight different specimens. Results from first and second analyses were compared by statistical analysis.

## GEOMAGIC CROSS-SECTION

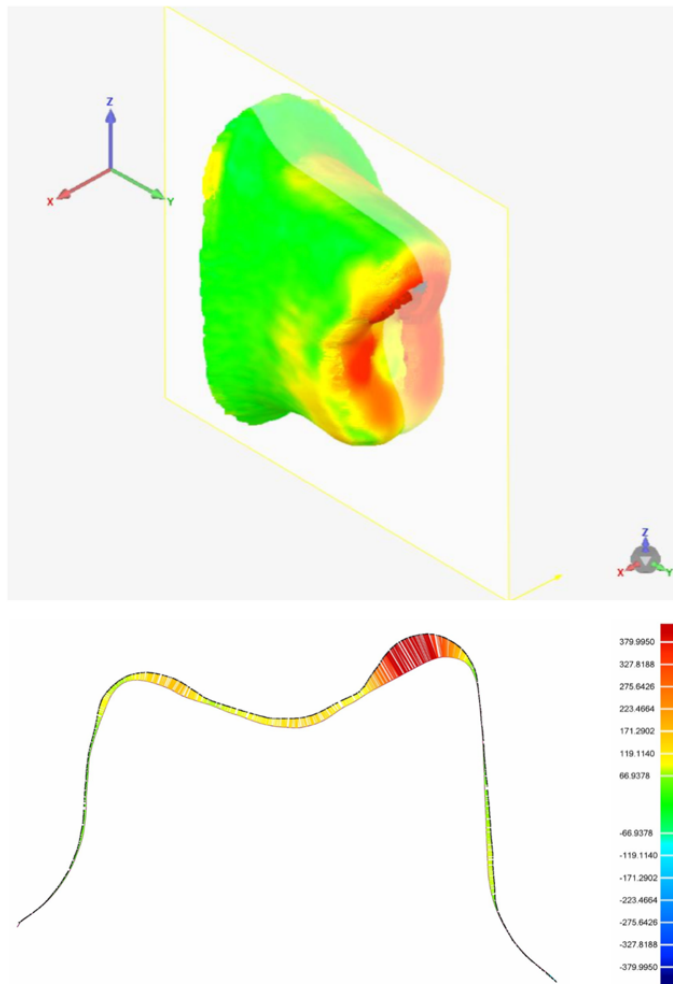


**FIGURE 31: GEOMAGIC CROSS-SECTION**



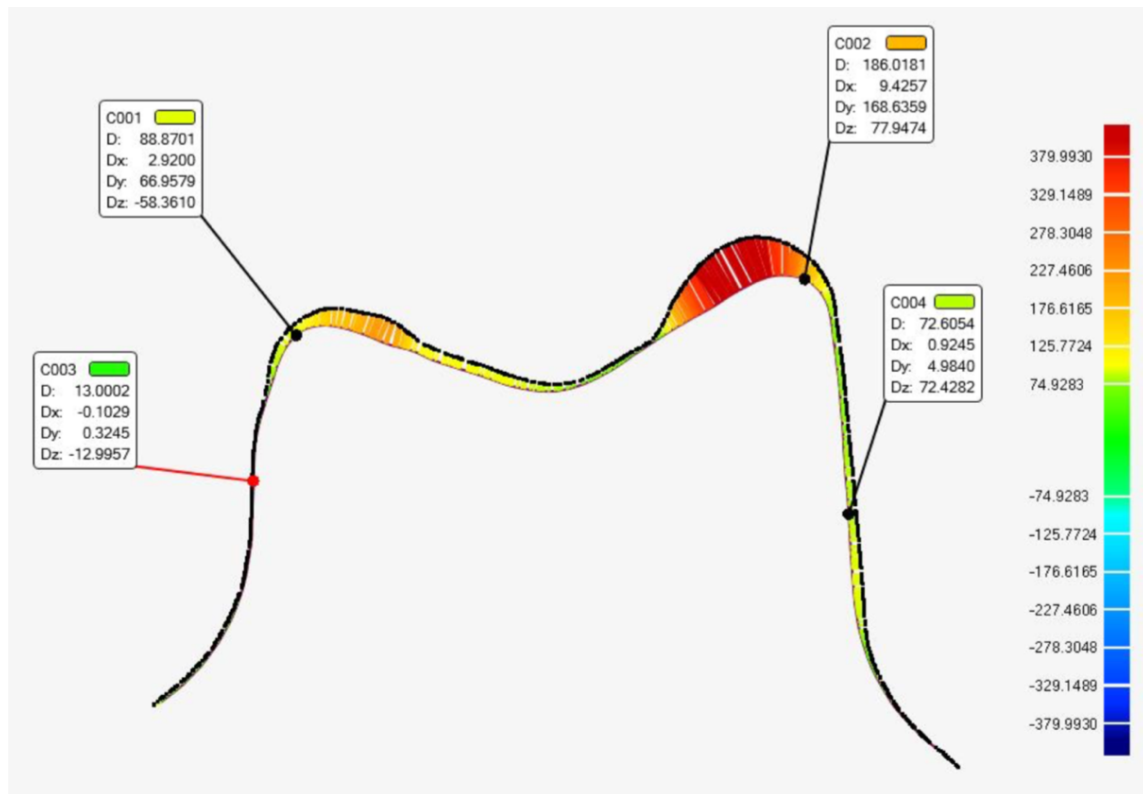


**FIGURE 32: GEOMAGIC CROSS-SECTION WITH MEASUREMENT ANNOTATIONS**

## 2.7 Statistical Analysis

Raw data was gathered from both Geomagic and SEM analyses. Statistical analyses were completed with SPSS software (SPSS 19.0, SPSS Inc., Chicago, IL) to assess the difference between the three groups. Kruskal-Wallis tests were administered and a p-value of less than 0.05 was used as a criterion for statistical significance. Following Kruskal-Wallis, post-hoc Mann-Whitney tests were administered with a Bonferroni correction of  $p < 0.017$ , adjusting for multiple comparisons. The measurements evaluated were SEM mean marginal opening, SEM mean marginal gap, Geomagic mean marginal gap, and Geomagic mean internal fit. These measurements were used for group comparisons to identify groups with any statistically significant differences.

Statistical analyses were used to evaluate validity and repeatability of the Geomagic measuring technique. In order to validate the Geomagic measuring technique, the marginal gap averages of SEM and marginal gap averages of Geomagic were statistically compared for each group with a paired t-test. In addition, a total of fifty measurements, twenty-five 2D SEM and twenty-five 2D Geomagic measurements were taken at the same location of specimens from all three groups and were statistically compared with a paired t-test. Geomagic repeatability was evaluated by repeating the alignment and marginal gap measurement of eight difference specimens and comparing the first and second measurements using the paired t-test.

### 3. RESULTS

The results of Kruskal-Wallis and post-hoc Mann-Whitney test for SEM marginal opening indicated Group's 1 and 2 Atlantis workflows are significantly smaller than Group 3 Full Digital Splitfile Workflow (Table 1, Figure 33).

Table 1: Mean 2D SEM Marginal Opening of 3 Experimental Groups

Experimental Groups	N	Mean 2D SEM Marginal Gap in microns (SD)	Group Comparisons* (p-value)	Maximum/ Minimum/ Median in microns
Group 1 Interrupted Digital Atlantis	7	13.84 (9.57)	Group 3 (0.002)	30.65 / 11.52 / 17.71
Group 2 Full Digital Atlantis	7	11.18 (3.65)	Group 3 (0.002)	15.29 / 10.01 / 11.98
Group 3 Full Digital Split-File	7	37.60 (14.02)	Group 1 (0.002) Group 2 (0.002)	58.91 / 35.32 / 47.84

\*Group with which experimental group was found to be significantly different from

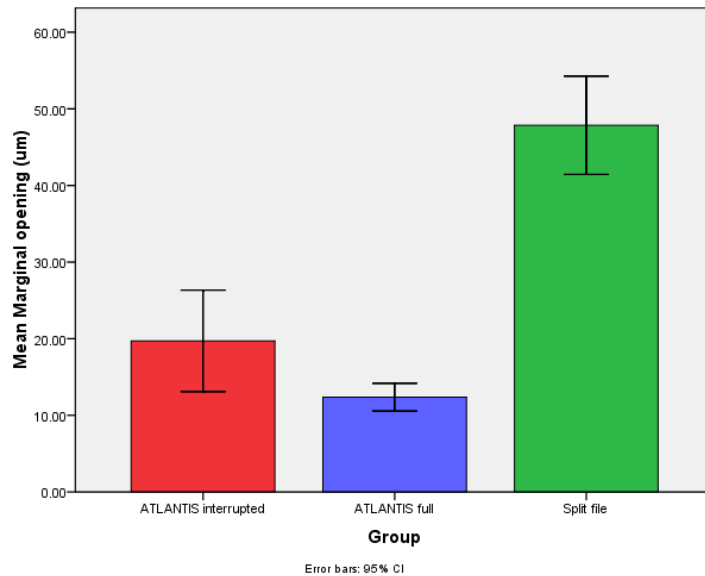


**FIGURE 33: 2D SEM MEAN MARGINAL OPENING COMPARISON OF 3 GROUPS**

The results of Kruskal-Wallis and post-hoc Mann-Whitney tests for both SEM and Geomagic marginal gap averages both indicated that the mean marginal gap for Group 2 Full Digital Atlantis Workflow is significantly smaller than the average marginal gaps of the other two groups (Table 2 & 3, Figure 34).

Table 2: Mean 2D SEM Marginal Gap of 3 Experimental Groups

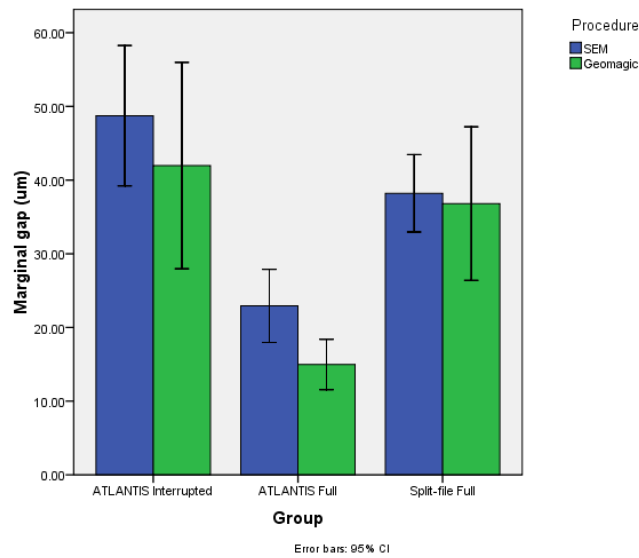
Experimental Groups	N	Mean 2D SEM Marginal Gap in microns (SD)	Group Comparisons* (p-value)	Maximum/ Minimum/ Median in microns
Group 1 Interrupted Digital Atlantis	7	48.73 (10.29)	Group 2 (0.002)	63.68 / 36.46 / 45.72
Group 2 Full Digital Atlantis	7	22.93 (5.36)	Group 1 (0.002) Group 3 (0.002)	28.65 / 14.14 / 25.14
Group 3 Full Digital Split-File	7	38.20 (5.67)	Group 2 (0.002)	47.64 / 31.95 / 37.13

\*Group with which experimental group was found to be significantly different from

Table 3: Mean 3D Geomagic Marginal Gap of 3 Experimental Groups

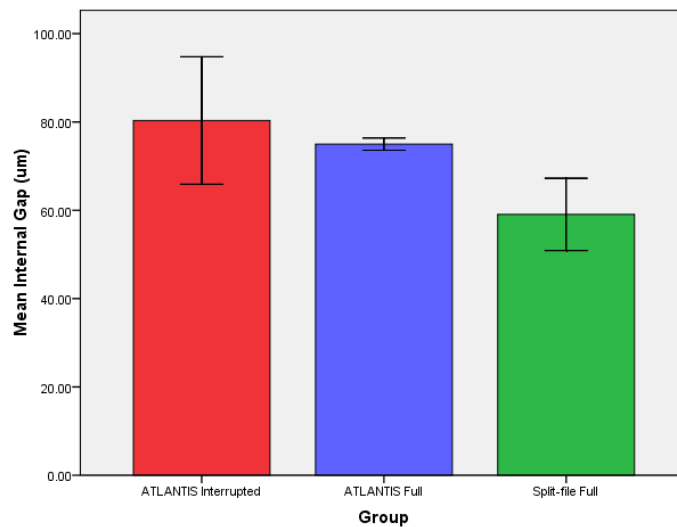
Experimental Groups	N	Mean 3D Geomagic Marginal Gap in microns (SD)	Group Comparisons* (p-value)	Maximum/ Minimum/ Median in microns
Group 1 Interrupted Digital Atlantis	6	41.96 (13.34)	Group 2 (0.004)	58.65 / 23.29 / 41.02
Group 2 Full Digital Atlantis	6	14.97 (3.25)	Group 1 (0.004) Group 3 (0.006)	17.67 / 10.11 / 16.34
Group 3 Full Digital Split-File	5	36.80 (8.39)	Group 2 (0.006)	44.18 / 24.29 / 38.93

\*Group with which experimental group was found to be significantly different from



**FIGURE 34: 2D SEM MEAN MARGINAL GAP VS 3D GEOMAGIC MEAN MARGINAL GAP COMPARISON OF 3 GROUPS**

The results of Kruskal-Wallis and post-hoc Mann-Whitney test for Geomagic overall internal fit indicated that mean internal fit for Group 3 Full Digital Split-File group was significantly smaller than the other two groups (Table 4, Figure 35).



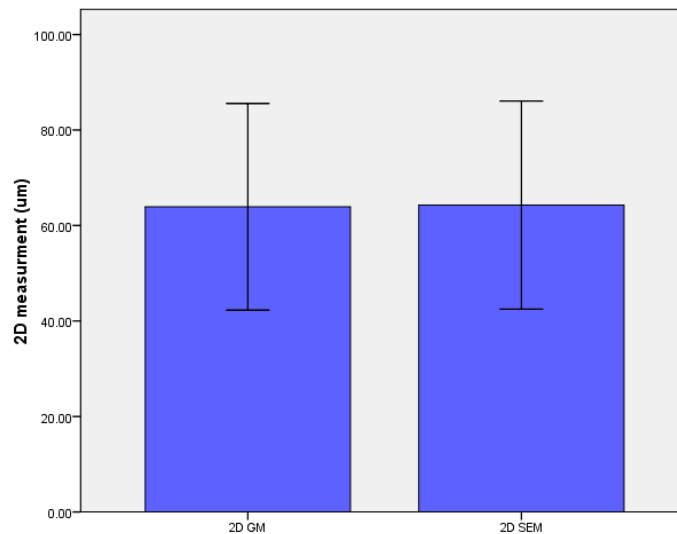
**FIGURE 35: 3D GEOMAGIC MEAN INTERNAL FIT COMPARISON OF 3 GROUPS**

Table 4: Mean 3D Geomagic Internal Fit of 3 Experimental Groups

Experimental Groups	N	Mean 3D Geomagic Internal Fit in microns (SD)	Group Comparisons* (p-value)	Maximum/ Minimum/ Median in microns
Group 1 Interrupted Digital Atlantis	6	80.33 (13.76)	Group 3 (0.006)	102.80 / 68.44 / 74.66
Group 2 Full Digital Atlantis	6	74.98 (1.32)	Group 3 (0.006)	76.65 / 73.19 / 74.61
Group 3 Full Digital Split-File	5	59.05 (6.59)	Group 1 (0.006) Group 2 (0.006)	65.15 / 48.44 / 61.78

\*Group with which experimental group was found to be significantly different from

Geomagic was validated by two statistical analyses. The results of the paired t-test completed for twenty-five 2D SEM and twenty-five 2D Geomagic sections taken at the same location of specimens from all three groups indicated no statistical difference amongst measurements for all three groups (Figure 36). Results of the paired t-test used to compare SEM mean marginal gap and Geomagic mean marginal gap indicated no statistically significant differences in measuring techniques (Table 5).



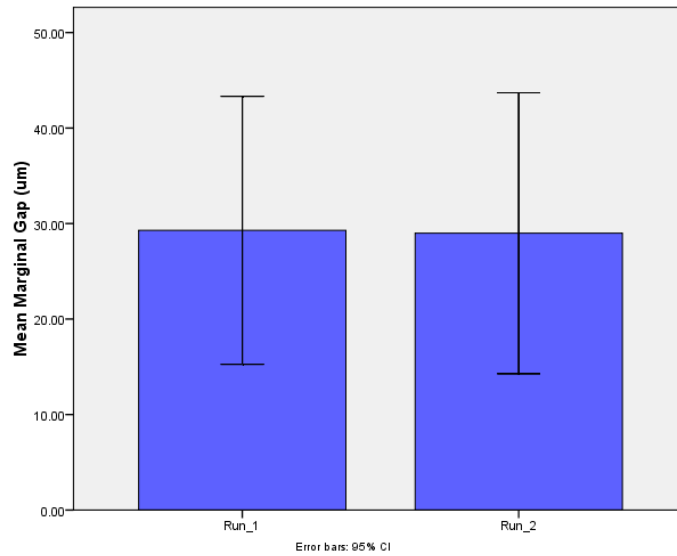
**FIGURE 36: 2D GEOMAGIC (GM) POINT MEASUREMENT VS 2D SEM POINT MEASUREMENT**

Table 5: Paired t-test p-values for Comparison of 2D SEM Mean Marginal Gap Compared to 3D Geomagic Mean Marginal Gap

Experimental Groups	N	p-value*
Group 1 Interrupted Digital Atlantis	6	0.221
Group 2 Full Digital Atlantis	6	0.066
Group 3 Full Digital Split-File	5	0.981

\*All three groups showed no significant statistical difference from one another (statistical significance =  $p < 0.05$ )

Geomagic repeatability was evaluated by comparing repeated marginal gap measurements taken from the same specimens. The results of the paired t-test that compared first and second 3D Geomagic marginal gap measurements of eight different specimens indicated no statistical difference between measurements for all eight specimens (Figure 37).



**FIGURE 37: FIRST GEOMAGIC MEASUREMENT (RUN\_1) VS SECOND GEOMAGIC MEASUREMENT (RUN\_2) FOR GEOMAGIC REPEATABILITY COMPARISON**

## 4. DISCUSSION

Results from this study indicate that all three workflows are clinically acceptable, as the average marginal gap assessed in each of the workflows is well below the clinically acceptable marginal opening of 120 microns used for this study. Therefore, regardless of statistical significance between groups, all three groups are well within the realm of clinical acceptability.

The accuracy of full digital workflows with digital design and milling of both a crown and custom abutment from a single .STL has only been studied once in the literature.<sup>33</sup> No previous studies in the literature have assessed internal fit and marginal gap of the two Atlantis digital workflows in this study. Therefore, this study provided information regarding accuracy in terms of marginal and internal fit, which can be used to determine clinical acceptability.

Digital dentistry has rapidly grown over the past several years. Although certain aspects of this new enterprise can certainly be used to ease some of the burdens clinicians and labs face, it can also be extremely complex and frustrating. Complications or confusion often arise due to the proprietary nature of different companies, in addition to closed architectures, or lack of proper integration of open architectures. In addition, open architecture software and their algorithms' significantly vary, and can therefore create questions regarding accuracy when combining them to create different workflows. The purpose of this study was to begin the very arduous task of verifying the accuracy of some of these workflows.

Although all clinically acceptable, comparison of marginal opening as measured



from SEM measurements revealed the two Atlantis workflows had significantly smaller marginal openings as compared to the Split-File Workflow. Statistical comparison of mean marginal gap for both SEM and Geomagic measurements between the three groups revealed the Full Digital Atlantis Workflow had a significantly smaller marginal gap than the other two groups. Smaller marginal opening and marginal gap decrease the likelihood of cement layer dissolution, gingival inflammation and other complications.<sup>36-41</sup>

An interesting finding of the study was the very small measurement deviations recorded for Full Digital Atlantis Workflow when compared to the other groups for all four comparisons (Tables 1-4, Figures 33-35). This smaller deviation suggests a greater degree of precision as compared to the other workflows. The standard deviation was greatest for Interrupted Digital Atlantis Workflow for three out of the four comparisons (Tables 2-4, Figures 34-35). It is possible that this increased variation may be due to the intermediate step and the potential inaccuracy it creates. In order to re-scan a titanium abutment, it must be coated with a spray to reduce reflectivity of the abutment in the scanner. The required use of spray to reduce reflectivity for most dental scanners is something to consider when utilizing the interrupted workflow. Coating sprays vary in application and thickness and therefore have the potential to alter the shape or thickness of the unit being scanned.

The Split-File Workflow showed the smallest internal fit compared to Atlantis groups (Table 4). Upon evaluation of the internal fit, this could potentially be due to the decreased occlusal cement space by-way of design of the Split-File group compared to the two Atlantis groups. The same experienced lab technician was used to design all crowns

for the Interrupted Atlantis and Full Digital Atlantis Workflows. A different experienced technician was used to design abutment and crown from the Split-File Workflow. Slight differences in settings or design could account for the variation in internal fit amongst the groups. In addition, the Atlantis abutment design included sharper line angles along the cusp heights of contour. The split-file abutment design could not be designed exactly the same as the Atlantis abutment due to required height of the titanium base, therefore the transition from the cusp height of contour to the mid-occlusal surface was less steep. The drill compensation offset and drill radius settings and milling could account for the larger occlusal cement space of the Atlantis groups compared to the split-file group.

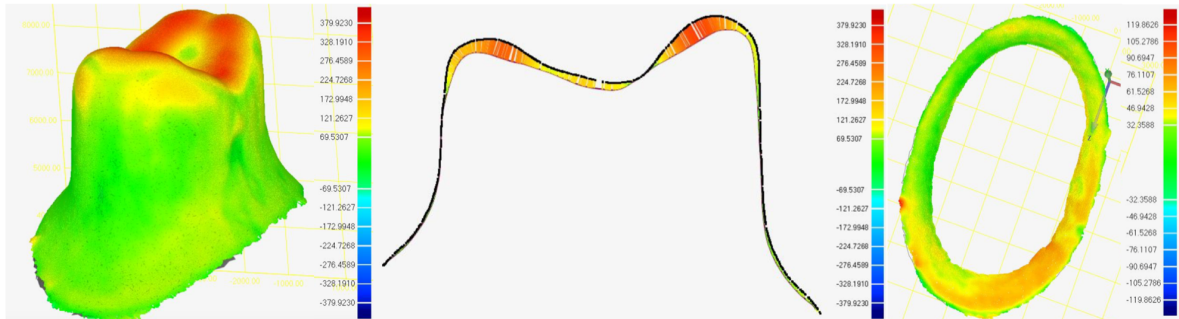
The study by Sheridan et al<sup>33</sup> is the only previous study to assess the split-file Workflow. For the full digital split-file workflow, Sheridan found, after adjustments, the mean marginal gap to be 69µm. This previous study assessed the split-file workflows against more traditional interrupted workflows, similar to the current study. Although the mean marginal gap of 69µm was within the realm of clinical acceptability, it was the largest marginal gap of all workflows within the study. The current study found a smaller mean marginal opening and mean marginal gap ranging from 36-38 µm. In addition, the previous study required several adjustments to the crowns in order to fully seat the crowns on the abutments. The current study required no adjustments for crown seating. This could potentially be due to the differences in materials used, differences in milling units, or the differences in cement space settings or drill compensation offset entered into the design software. Regardless, both the previous and current studies found mean marginal gaps clinically acceptable.

The results of this study have significant clinical relevance and applicability. These clinically acceptable results indicate that the full digital workflows utilized in this study can be used with reliability in practice, reducing number of appointments, time, and cost. However, the Atlantis interrupted digital workflow is also clinically acceptable, allowing clinicians to choose which workflow is the best fit for the clinical situation.

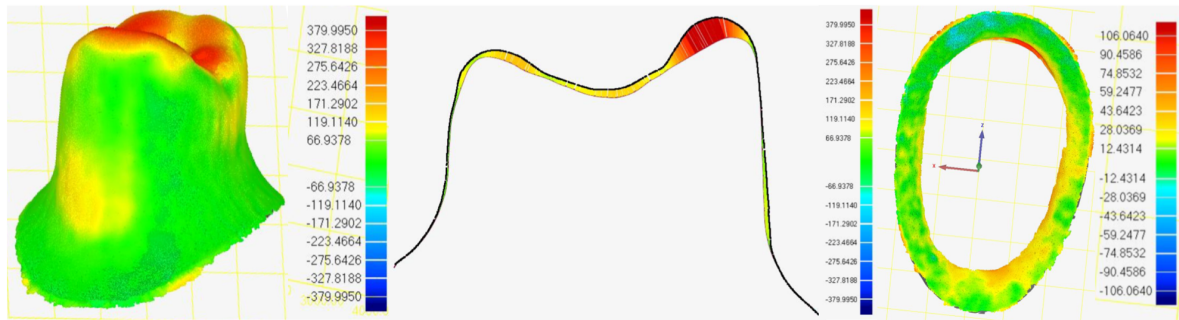
One major advantage of this study was the use of Geomagic and its' capabilities, allowing for visualization and measurement at virtually any position. Geomagic enabled 3D measurements of the entire internal fit, the marginal gap, and 2D sections for each specimen (Figure 38). Groten et al<sup>46</sup> determined that a minimum of fifty measurements are required to determine marginal gap. The Geomagic measurement protocol used within this study resulted in an averaged 197,000 points of measurement for internal fit of each sample and averaged 57,000 points of measurement around the marginal gap. With other forms of non-digital measurement, it would be impossible to collect this many data points. In addition, its' nondestructive nature allows further use and evaluation of the crowns and abutments.

As previously stated, the Geomagic measuring technique in this study was validated in several ways comparing 2D measurements acquired by SEM with 2D and 3D Geomagic measurements. A total of fifty measurements, twenty-five 2D SEM and twenty-five 2D Geomagic measurements, were statistically compared with a paired t-test and the differences of all twenty-five pairs of measurements compared were found to not be significantly different. In addition, averaged marginal gaps were statistically compared

### GROUP 1 ATLANTIS INTERRUPTED DIGITAL WORKFLOW



### GROUP 2 ATLANTIS FULL DIGITAL WORKFLOW



### GROUP 3 SPLIT-FILE FULL DIGITAL WORKFLOW

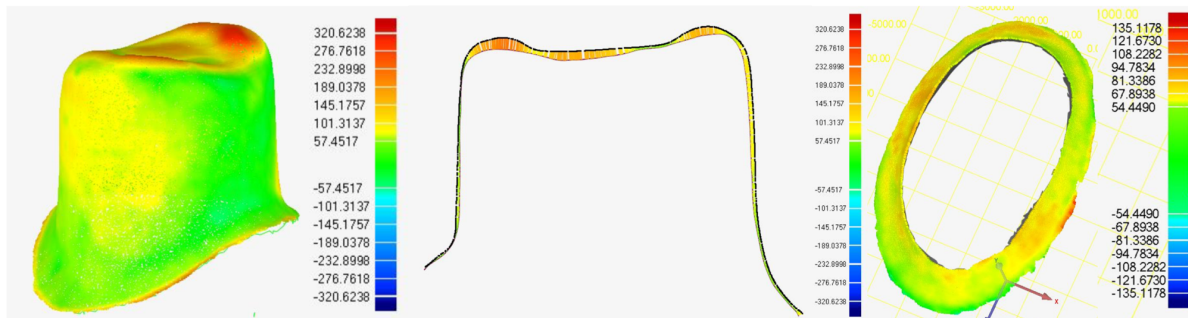


**FIGURE 38: GEOMAGIC 3D & 2D ANALYSIS OF EACH GROUP**

between the two measuring techniques and had no statistical difference. To demonstrate repeatability, alignment and marginal gap averages were repeated on the same specimen with eight different specimens and results between the first and second measurements were compared with paired t-test. No statistically significant difference was found between any of the eight duplicate measurements, illustrating reliable repeatability.

A possible limitation or source of error for the study includes the use of spray to reduce reflectivity prior to scanning the titanium abutments. Another limitation may be scan alignment error associated with the Geomagic measuring technique. Alignment error, or deviation, had a positive average of 6 microns or less and RMS estimate of 12 microns or less for each specimen analyzed. These values were determined from a pilot study as the maximum allowable alignment deviation values while still arriving at accurate data. In order to minimize error due to software alignment, any aligned specimens with a positive deviation of more than 6 microns or RMS estimate of greater than 12 microns were re-aligned until a smaller deviation was obtained, or the specimen was eliminated from the data. In addition to Geomagic alignment error, there was also the potential for error from the lab scanner. The D900 has a precision of 8 microns.

Another limitation of the study could be the possibility of the PVS slightly lifting away from the abutment surface, which may be imperceptible to the eye but could slightly alter final measurements. Also, the number of samples per group in this study were relatively small. Not all specimens used for SEM analysis were available for Geomagic analysis. One specimen from each group was sent for SEM sectioning prior to the protocol for the Geomagic measuring technique was developed. In addition, one specimen from the

Split-File workflow failed an accurate alignment, therefore results were not included in the final Geomagic measurements. Regardless, results still indicated a statistical difference for both the SEM and Geomagic analyses, and clinically acceptable results for all three workflows. It is unlikely the lack of 3D measurements obtained created any difference in the overall outcomes of the study.

Further studies are recommended to continue evaluating the wide array of digital workflows now available.

## 5. CONCLUSIONS

Within the limitations of this in vitro study the following conclusions can be drawn:

1. All three workflows evaluated in this study show clinically acceptable results in terms of mean marginal gap below 120 microns.
2. SEM evaluation of mean marginal opening revealed Interrupted Digital Atlantis Workflow and Full Digital Atlantis Workflow mean marginal openings were statistically smaller when compared to the Full Digital Split-File Workflow.
3. SEM and Geomagic measurements revealed Full Digital Atlantis Workflow mean marginal gap was significantly smaller when compared to Interrupted Digital Atlantis Workflow and Full Digital Split-file Workflow.
4. Geomagic evaluation of mean internal fit revealed Full Digital Split-File Workflow was significantly smaller when compared to Interrupted Digital Atlantis Workflow and Full Digital Atlantis Workflow.
5. The use of Geomagic to measure and evaluate mean marginal gap and mean internal fit as defined within this study proved to be an acceptable form of measurement per it's statistical validation herein.

## REFERENCES

1. Kapos T, Evans C. CAD/CAM technology for implant abutments, crowns, and superstructures. *Int J Oral Maxillofac Implants* 2014;29 Suppl:117-136.
2. Kim KB, Kim JH, Kim WC, Kim JH. Three-dimensional evaluation of gaps associated with fixed dental prostheses fabricated with new technologies. *J Prosthet Dent* 2014;112:1432-1436.
3. Ng J, Ruse D, Wyatt C. A comparison of the marginal fit of crowns fabricated with digital and conventional methods. *J Prosthet Dent* 2014;112:555-560.
4. Brandt J, Lauer HC, Peter T, Brandt S. Digital process for an implant-supported fixed dental prosthesis: A clinical report. *J Prosthet Dent* 2015;114:469-473.
5. Joda T, Bragger U. Time-Efficiency Analysis Comparing Digital and Conventional Workflows for Implant Crowns: A Prospective Clinical Crossover Trial. *Int J Oral Maxillofac Implants* 2015;30:1047-1053.
6. Rompen E. The impact of the type and configuration of abutments and their (repeated) removal on the attachment level and marginal bone. *Eur J Oral Implantol* 2012;5 Suppl:S83-90.
7. Blatz MBaG, Inaki *EVOLUTION: Contemporary Protocols for Anterior Single-Tooth Implants*: Quintessence Publishing; 2014.
8. Hermann JS, Schoolfield JD, Schenk RK, Buser D, Cochran DL. Influence of the size of the microgap on crestal bone changes around titanium implants. A histometric evaluation of unloaded non-submerged implants in the canine mandible. *J Periodontol* 2001;72:1372-1383.



9. Abrahamsson I, Berglundh T, Lindhe J. The mucosal barrier following abutment dis/reconnection. An experimental study in dogs. *J Clin Periodontol* 1997;24:568-572.
10. Hinds KF. Custom impression coping for an exact registration of the healed tissue in the esthetic implant restoration. *Int J Periodontics Restorative Dent* 1997;17:584-591.
11. Papadopoulos I, Pozidi G, Goussias H, Kourtis S. Transferring the emergence profile from the provisional to the final restoration. *J Esthet Restor Dent* 2014;26:154-161.
12. Furze D, Byrne A, Donos N, Mardas N. Clinical and esthetic outcomes of single-tooth implants in the anterior maxilla. *Quintessence Int* 2012;43:127-134.
13. Ferrari M, Tricarico MG, Cagidiaco MC, et al. 3-Year Randomized Controlled Prospective Clinical Trial on Different CAD-CAM Implant Abutments. *Clin Implant Dent Relat Res* 2016;18:1134-1141.
14. [www.dentsply.com](http://www.dentsply.com). ATLANTIS Core File. Available at:  
<https://www.dentsply.com/en-uk/implants.html/products/Implants/Digital-solutions/ATLANTIS%E2%84%A2-abutments/Patient-specific-abutments/ATLANTIS-Abutment-Core-File/p/IMP-TEMP-013.html>. 2016.
15. Nakamura K, Kanno T, Milleding P, Ortengren U. Zirconia as a dental implant abutment material: a systematic review. *Int J Prosthodont* 2010;23:299-309.

16. Raigrodski AJ, Hillstead MB, Meng GK, Chung KH. Survival and complications of zirconia-based fixed dental prostheses: a systematic review. *J Prosthet Dent* 2012;107:170-177.
17. Sailer I, Philipp A, Zembic A, Pjetursson BE, Hammerle CH, Zwahlen M. A systematic review of the performance of ceramic and metal implant abutments supporting fixed implant reconstructions. *Clin Oral Implants Res* 2009;20 Suppl 4:4-31.
18. Zembic A, Kim S, Zwahlen M, Kelly JR. Systematic review of the survival rate and incidence of biologic, technical, and esthetic complications of single implant abutments supporting fixed prostheses. *Int J Oral Maxillofac Implants* 2014;29 Suppl:99-116.
19. Ekfeldt A, Furst B, Carlsson GE. Zirconia abutments for single-tooth implant restorations: a retrospective and clinical follow-up study. *Clin Oral Implants Res* 2011;22:1308-1314.
20. Ichikawa Y, Akagawa Y, Nikai H, Tsuru H. Tissue compatibility and stability of a new zirconia ceramic in vivo. *J Prosthet Dent* 1992;68:322-326.
21. Rimondini L, Cerroni L, Carrassi A, Torricelli P. Bacterial colonization of zirconia ceramic surfaces: an in vitro and in vivo study. *Int J Oral Maxillofac Implants* 2002;17:793-798.
22. Scarano A, Piattelli M, Caputi S, Favero GA, Piattelli A. Bacterial adhesion on commercially pure titanium and zirconium oxide disks: an in vivo human study. *J Periodontol* 2004;75:292-296.

23. Welander M, Abrahamsson I, Berglundh T. The mucosal barrier at implant abutments of different materials. *Clin Oral Implants Res* 2008;19:635-641.
24. Jung RE, Sailer I, Hammerle CH, Attin T, Schmidlin P. In vitro color changes of soft tissues caused by restorative materials. *Int J Periodontics Restorative Dent* 2007;27:251-257.
25. Chevalier J. What future for zirconia as a biomaterial? *Biomaterials* 2006;27:535-543.
26. Ferrari M, Vichi A, Zarone F. Zirconia abutments and restorations: from laboratory to clinical investigations. *Dent Mater* 2015;31:e63-76.
27. Kim A, Campbell SD, Viana MA, Knoernschild KL. Abutment Material Effect on Peri-implant Soft Tissue Color and Perceived Esthetics. *J Prosthodont* 2016;25:634-640.
28. Gehrke P, Johansson D, Fischer C, Stawarczyk B, Beuer F. In vitro fatigue and fracture resistance of one- and two-piece CAD/CAM zirconia implant abutments. *Int J Oral Maxillofac Implants* 2015;30:546-554.
29. de Franca DG, Morais MH, das Neves FD, Barbosa GA. Influence of CAD/CAM on the fit accuracy of implant-supported zirconia and cobalt-chromium fixed dental prostheses. *J Prosthet Dent* 2015;113:22-28.
30. Bosch G, Ender A, Mehl A. A 3-dimensional accuracy analysis of chairside CAD/CAM milling processes. *J Prosthet Dent* 2014;112:1425-1431.

31. Lins L, Bemfica V, Queiroz C, Canabarro A. In vitro evaluation of the internal and marginal misfit of CAD/CAM zirconia copings. *J Prosthet Dent* 2015;113:205-211.
32. Ha SJ, Cho JH. Comparison of the fit accuracy of zirconia-based prostheses generated by two CAD/CAM systems. *J Adv Prosthodont* 2016;8:439-448.
33. Sheridan RR, Haney, S, et al. Effect of Split-File Digital Workflow on Crown Margin Adaptation. *Journal of Prosthodontics* 2017;doi: 10.1111/jopr.12606.
34. Evan Kemper, Whipmix. 3Shape Quick Tip: Split File Designing. Available at: <http://info.whipmix.com/3shape-quick-tip-split-file-designing>.
35. The Split File Technique: Minimizes Turnaround, Maximizes Efficiency. Available at: <http://lmtmag.com/articles/the-split-file-technique-minimizes-turnaround-maximizes-efficiency>. 2017.
36. Torabi Ardekani K, Ahangari AH, Farahi L. Marginal and internal fit of CAD/CAM and slip-cast made zirconia copings. *J Dent Res Dent Clin Dent Prospects* 2012;6:42-48.
37. Rekow ED, Zhang G, Thompson V, Kim JW, Coehlo P, Zhang Y. Effects of geometry on fracture initiation and propagation in all-ceramic crowns. *J Biomed Mater Res B Appl Biomater* 2009;88:436-446.
38. Felton DA, Kanoy BE, Bayne SC, Wirthman GP. Effect of in vivo crown margin discrepancies on periodontal health. *J Prosthet Dent* 1991;65:357-364.
39. Orstavik D, Orstavik J. In vitro attachment of *Streptococcus sanguis* to dental crown and bridge cements. *J Oral Rehabil* 1976;3:139-144.

40. Silness J, Hegdahl T. Area of the exposed zinc phosphate cement surfaces in fixed restorations. *Scand J Dent Res* 1970;78:163-177.
41. Jacobs MS, Windeler AS. An investigation of dental luting cement solubility as a function of the marginal gap. *J Prosthet Dent* 1991;65:436-442.
42. Holmes JR, Bayne SC, Holland GA, Sulik WD. Considerations in measurement of marginal fit. *J Prosthet Dent* 1989;62:405-408.
43. Sorensen JA. A standardized method for determination of crown margin fidelity. *J Prosthet Dent* 1990;64:18-24.
44. Seker E, Ozcelik TB, Rath N, Yilmaz B. Evaluation of marginal fit of CAD/CAM restorations fabricated through cone beam computerized tomography and laboratory scanner data. *J Prosthet Dent* 2016;115:47-51.
45. Euan R, Figueras-Alvarez O, Cabratosa-Termes J, Oliver-Parra R. Marginal adaptation of zirconium dioxide copings: influence of the CAD/CAM system and the finish line design. *J Prosthet Dent* 2014;112:155-162.
46. Groten M, Axmann D, Probst L, Weber H. Determination of the minimum number of marginal gap measurements required for practical in-vitro testing. *J Prosthet Dent* 2000;83:40-49.
47. Anadioti E, Aquilino SA, Gratton DG, et al. 3D and 2D marginal fit of pressed and CAD/CAM lithium disilicate crowns made from digital and conventional impressions. *J Prosthodont* 2014;23:610-617.

48. Holst S, Karl M, Wichmann M, Matta RE. A technique for in vitro fit assessment of multi-unit screw-retained implant restorations: Application of a triple-scan protocol. *J Dent Biomech* 2012;3:1758736012452181.
49. Alfaro DP, Ruse ND, Carvalho RM, Wyatt CC. Assessment of the Internal Fit of Lithium Disilicate Crowns Using Micro-CT. *J Prosthodont* 2015;24:381-386.
50. Luthardt RG, Bornemann G, Lemelson S, Walter MH, Huls A. An innovative method for evaluation of the 3-D internal fit of CAD/CAM crowns fabricated after direct optical versus indirect laser scan digitizing. *Int J Prosthodont* 2004;17:680-685.
51. Moldovan O, Luthardt RG, Corcodel N, Rudolph H. Three-dimensional fit of CAD/CAM-made zirconia copings. *Dent Mater* 2011;27:1273-1278.
52. Holst S, Karl M, Wichmann M, Matta RE. A new triple-scan protocol for 3D fit assessment of dental restorations. *Quintessence Int* 2011;42:651-657.
53. Christensen GJ. Marginal fit of gold inlay castings. *J Prosthet Dent* 1966;16:297-305.
54. McLean JW, von Fraunhofer JA. The estimation of cement film thickness by an in vivo technique. *Br Dent J* 1971;131:107-111.
55. Martinez-Rus F, Ferreiroa A, Ozcan M, Pradies G. Marginal discrepancy of monolithic and veneered all-ceramic crowns on titanium and zirconia implant abutments before and after adhesive cementation: a scanning electron microscopy analysis. *Int J Oral Maxillofac Implants* 2013;28:480-487.

56. Brusco N, Andreetto M, Lucchese L, Carmignato S, Cortelazzo GM. Metrological validation for 3D modeling of dental plaster casts. *Med Eng Phys* 2007;29:954-966.
57. Martorelli M, Ausiello P, Morrone R. A new method to assess the accuracy of a Cone Beam Computed Tomography scanner by using a non-contact reverse engineering technique. *J Dent* 2014;42:460-465.
58. Luthardt RG, Kuhmstedt P, Walter MH. A new method for the computer-aided evaluation of three-dimensional changes in gypsum materials. *Dent Mater* 2003;19:19-24.
59. Luthardt RG, Loos R, Quaas S. Accuracy of intraoral data acquisition in comparison to the conventional impression. *Int J Comput Dent* 2005;8:283-294.
60. Solaberrieta E, Otegi JR, Goicoechea N, Brizuela A, Pradies G. Comparison of a conventional and virtual occlusal record. *J Prosthet Dent* 2015;114:92-97.
61. Levine WA. An evaluation of the film thickness of resin luting agents. *J Prosthet Dent* 1989;62:175-178.
62. Tamim H, Skjerven H, Ekfeldt A, Ronold HJ. Clinical evaluation of CAD/CAM metal-ceramic posterior crowns fabricated from intraoral digital impressions. *Int J Prosthodont* 2014;27:331-337.
63. Molin M, Karlsson S. The fit of gold inlays and three ceramic inlay systems. A clinical and in vitro study. *Acta Odontol Scand* 1993;51:201-206.

64. Rahme HY, Tehini GE, Adib SM, Ardo AS, Rifai KT. In vitro evaluation of the "replica technique" in the measurement of the fit of Procera crowns. *J Contemp Dent Pract* 2008;9:25-32.
65. Boening KW, Wolf BH, Schmidt AE, Kastner K, Walter MH. Clinical fit of Procera AllCeram crowns. *J Prosthet Dent* 2000;84:419-424.
66. Martins LM, Lorenzoni FC, Melo AO, et al. Internal fit of two all-ceramic systems and metal-ceramic crowns. *J Appl Oral Sci* 2012;20:235-240.
67. Kokubo Y, Ohkubo C, Tsumita M, Miyashita A, Vult von Steyern P, Fukushima S. Clinical marginal and internal gaps of Procera AllCeram crowns. *J Oral Rehabil* 2005;32:526-530.
68. Lee DH. Digital approach to assessing the 3-dimensional misfit of fixed dental prostheses. *J Prosthet Dent* 2016;116:836-839.
69. Ortega R, Gonzalo E, Gomez-Polo M, Suarez MJ. Marginal and Internal Discrepancies of posterior zirconia-based crowns fabricated with three different CAD/CAM systems versus metal-ceramic. *Int J Prosthodont* 2015;28:509-511.
70. Apicella D, Veltri M, Chieffi N, Balleri P, Ferrari M. Cement thickness at implant-supported single-tooth Lava assemblies: a scanning electron microscopic investigation. *Clin Oral Implants Res* 2010;21:747-750.